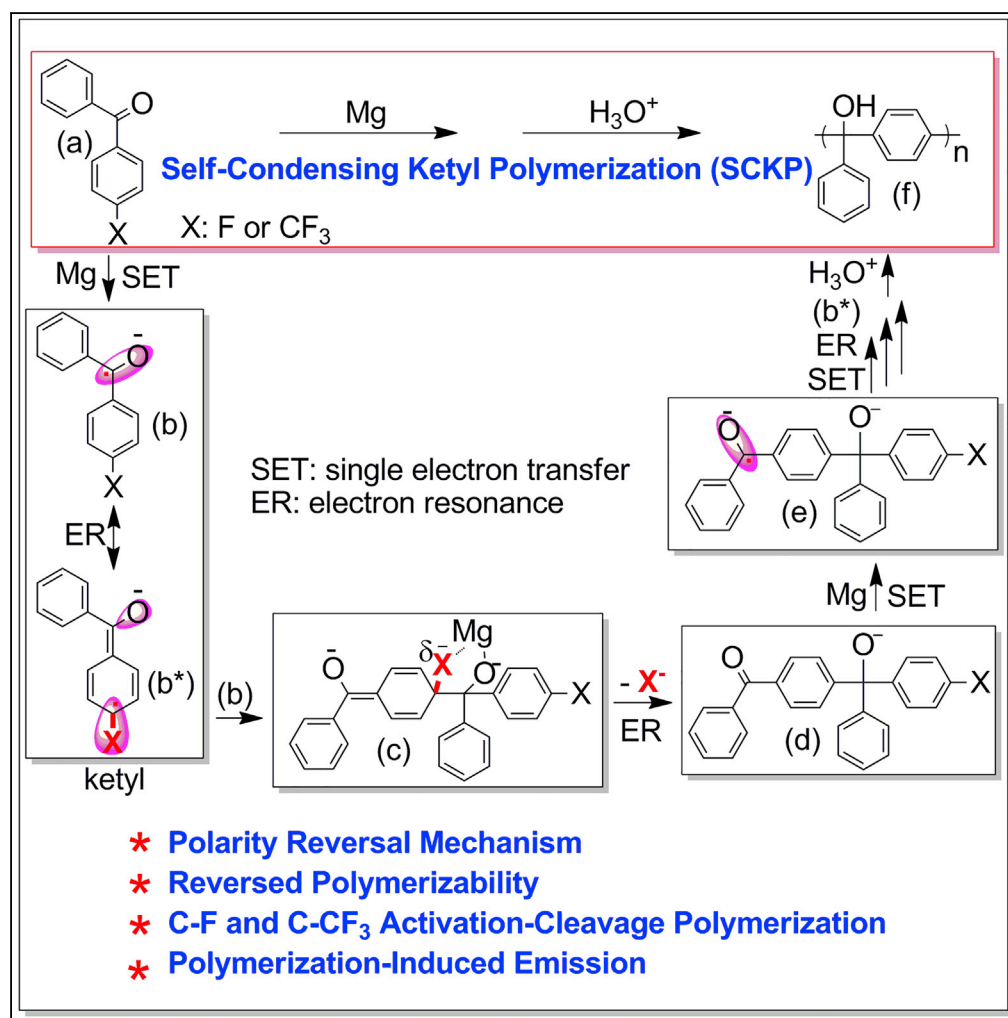


Article

Barbier Self-Condensing Ketyl Polymerization-Induced Emission: A Polarity Reversal Approach to Reversed Polymerizability



Shun-Shun Li,
 Nengbo Zhu, Ya-
 Nan Jing, Yajun Li,
 Hongli Bao, Wen-
 Ming Wan

wanwenming@fjirsm.ac.cn

HIGHLIGHTS

Self-condensing ketyl
 polymerization

Polymerization-induced
 emission

C-F/C-CF₃ activation
 polymerization

Polarity reversal and
 reversed polymerizability

Article

Barbier Self-Condensing Ketyl Polymerization-Induced Emission: A Polarity Reversal Approach to Reversed Polymerizability

Shun-Shun Li,^{1,2,3,4} Nengbo Zhu,^{1,2,4} Ya-Nan Jing,^{1,2,3,4} Yajun Li,^{1,2} Hongli Bao,^{1,2} and Wen-Ming Wan^{1,2,3,5,*}

SUMMARY

Carbon-carbon bond formation through polarity reversal ketyl radical anion coupling of carbonyls has inspired new reaction modes to this cornerstone carbonyl group and played significant roles in organic chemistry. The introduction of this resplendent polarity reversal ketyl strategy into polymer chemistry will inspire new polymerization mode with unpredicted discoveries. Here we show the successful introduction of polarity reversal ketyl approach to polymer chemistry to realize self-condensing ketyl polymerization with polymerization-induced emission. In this polarity reversal approach, it exhibits intriguing reversed polymerizability, where traditional excellent leaving groups are not suitable for polymerization but challenging polymerizations involving the cleavage of challenging C-F and C-CF₃ bonds are realized under mild Barbier conditions. This polarity reversal approach enables the polymer chemistry with polarity reversal ketyl mode, opens up a new avenue toward the polymerization of challenging C-X bonds under mild conditions, and sparks design inspiration of new reaction, polymerization, and functional polymer.

INTRODUCTION

Carbon-carbon (C-C) bond formation plays a central role in modern organic synthesis. In comparison with C-C bond formation through classic polar coupling mechanism, C-C bond formation through polarity reversal ketyl radical anion (ketyl) coupling of carbonyls enables access to a polarity-reversed platform with reactivity umpolung and has inspired new reaction modes to this cornerstone carbonyl group in organic chemistry (Hart, 1984; Wang et al., 2017, 2018). The development of new polymerization methodology based on this resplendent polarity reversal ketyl strategy will inspire new polymerization mode with unpredicted discoveries, expand the structure and functionality libraries of monomer and polymer, and open up a new avenue for the design and application of polymer materials.

Classical C-C bond formation reactions, including atom transfer radical addition reaction (Pintauer and Matyjaszewski, 2008; Wang and Matyjaszewski, 1995), radical addition-fragmentation reaction (Chieffari et al., 1998; Moad et al., 2008), olefin metathesis reaction (Bielawski and Grubbs, 2000, 2007; Vougioukalakis and Grubbs, 2010), Suzuki coupling reaction (Baggett et al., 2015; Kotha et al., 2002; Littke et al., 2000; Miyaura et al., 1981; Schluter, 2001; Yokoyama et al., 2007), Michael addition reaction (Hong et al., 2007; Liu et al., 2003; Wang et al., 2005), Stille coupling reaction (Bao et al., 1995; Guo et al., 2014; Littke and Fu, 1999; Yin et al., 2016), click chemistry reactions (He et al., 2016, 2017), multiple components reactions (Deng et al., 2012, 2016; Kreye et al., 2011; Wei et al., 2017; Wu et al., 2017; Xue et al., 2016), the Barbier reaction (Jing et al., 2019; Sun et al., 2017), and radical cascade reaction (Zhu et al., 2020), have been introduced to polymer chemistry to develop polymerization methodologies (Hawker and Wooley, 2005; Huang et al., 2019; Iha et al., 2009; Jiang et al., 2018; Song et al., 2018; Tsao and Wooley, 2017). Generally, C-C bond formation is initiated by activation-cleavage of C-X bonds, such as C-I, C-Br, C-Cl, C-S, C-O, and C-B, and these C-X bond activation-cleavage polymerizations have been well established in polymer chemistry with X as traditional leaving group. In comparison, both organic reaction and polymerization involving C-F or C-CF₃ bond activation-cleavage have not been well realized yet and are significantly challenging, taking Barbier reaction as an example (Figure 1A), (Berger et al., 2018; Blomberg, 1993; Blomberg and Hartog, 1977; Li and Zhang, 1998; Sergeev et al., 1982; Zhang and Li, 1999; Zhou and Li, 2014) stemming from

¹State Key Laboratory of Structural Chemistry, Key Laboratory of Coal to Ethylene Glycol and Its Related Technology, Center for Excellence in Molecular Synthesis, Fujian Institute of Research on the Structure of Matter, Chinese Academy of Sciences, 155 West Yangqiao Road, Fuzhou 350002, P. R. of China

²University of Chinese Academy of Sciences, Beijing 100049, P. R. of China

³State Key Laboratory of Heavy Oil Processing and Center for Bioengineering and Biotechnology, China University of Petroleum (East China), 66 West Changjiang Road, Qingdao 266580, P. R. of China

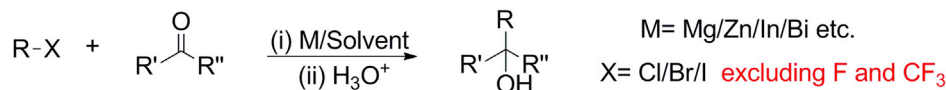
⁴These authors contributed equally

⁵Lead Contact

*Correspondence: wanwenming@fjirsm.ac.cn
<https://doi.org/10.1016/j.isci.2020.101031>



A Previous work (Reaction and polymerization involving C-F or C-CF₃ are challenging)



B This work (Polarity reversal approach)

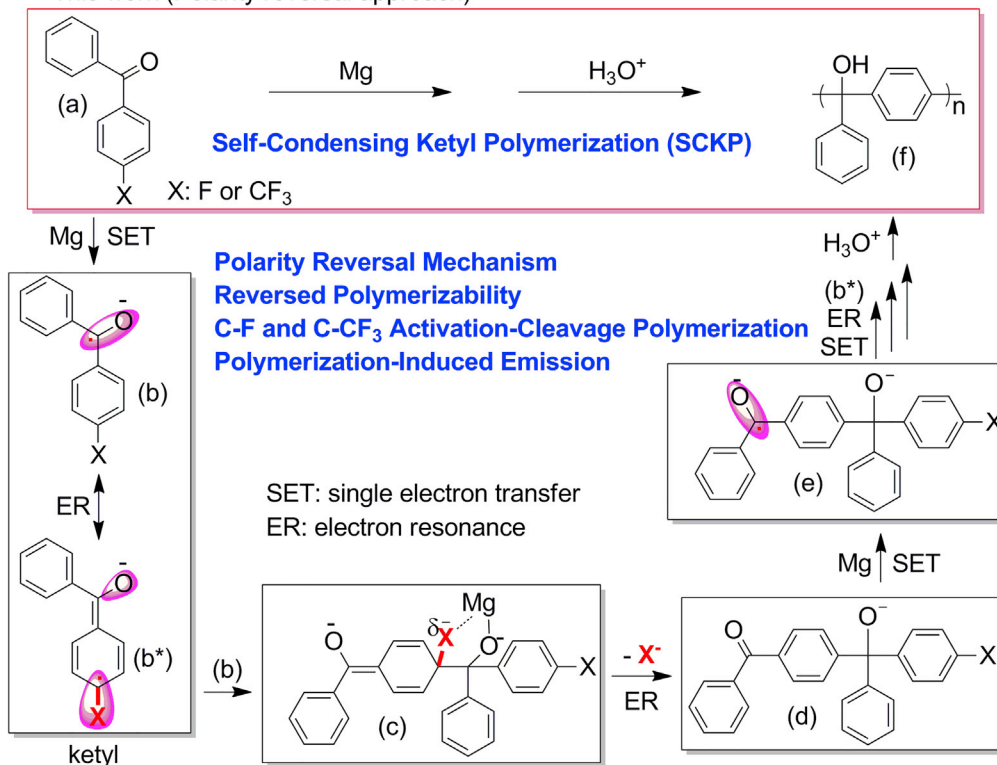


Figure 1. The Introduction of Polarity Reversal Ketyl Strategy into Polymer Chemistry

The introduction of polarity reversal ketyl strategy into polymer chemistry to realize self-condensing ketyl polymerization triggered by electron resonance, enabling reversed polymerizability toward C-F and C-CF₃ activation-cleavage polymerization. (A) Previous work of the Barbier reaction involving challenging C-F or C-CF₃. (B) Polarity reversal strategy via self-condensing ketyl polymerization in this work.

the extremely high bond dissociation energy (Ahrens et al., 2015; Amii and Uneyama, 2009; Cui et al., 2018; Meissner et al., 2017; Tian et al., 2015).

Owing to the high bond dissociation energy of the C-F and C-CF₃ bonds, activation-cleavage of these bonds through direct insertion of Mg into the C-F or C-CF₃ bond is difficult. Taking C-F activation-cleavage in Barbier reaction as an example, we hypothesize that, instead, Mg will react with the carbonyl group in the formation of ketyl through a reductive polarity reversal mechanism via single electron transfer (SET) and Mg will interact with C-F bond through van der Waals forces as well, resulting in nucleophilic addition of a ketyl to the C-F bond and formation of a five-membered ring intermediate (Figure S1). Mg-mediated C-F activation-cleavage and addition to a carbonyl group can therefore be realized in a one-pot Barbier reaction through polarity reversal ketyl mechanism. Furthermore, in the case of 4-fluorobenzophenone ([a] in Figure 1B), a SET between Mg and 4-fluorobenzophenone (a) will produce a ketyl (b) through reductive polarity reversal mechanism, where (b*) is another electron resonance (ER) structure of ketyl of (b). Self-condensing coupling between (b) and (b*) will initiate the self-condensing dimerization of ketyl, which involves formation of (c), cleavage of the C-F bond and ER in the formation of a carbonyl end group (d), and a SET between (d) and Mg forming a ketyl dimer (e). Continuous chain propagation with (b*) as monomer followed by ER and SET processes, Mg-mediated C-F activation-cleavage polymerization can be realized by polarity reversal strategy through self-condensing ketyl polymerization (SCKP) of (a), similar to the self-condensing

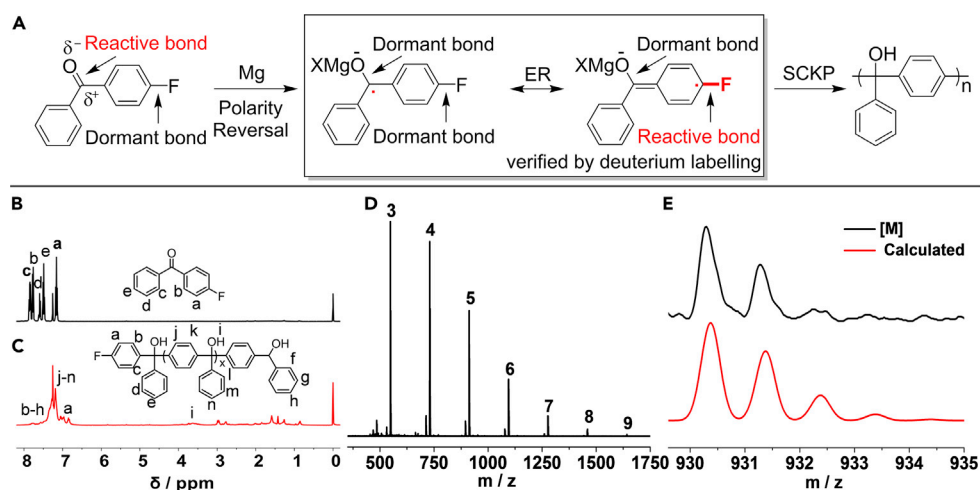


Figure 2. Process of Self-Condensing Ketyl Polymerization and Characterizations of Fluoro-poly(triphenylmethanol) (fluoro-PTPM) Synthesized with 4-fluorobenzophenone as Monomer

- (A) Proposed mechanism of self-condensing ketyl polymerization.
 (B) ^1H NMR spectrum of 4-fluorobenzophenone in CDCl_3 .
 (C) ^1H NMR spectrum of fluoro-PTPM in CDCl_3 .
 (D) Complete MALDI-TOF spectrum of fluoro-PTPM.
 (E) Comparison between observed and calculated MALDI-TOF mass spectra of pentamer [M].

concept of self-condensing vinyl polymerization proposed by Fréchet (Fréchet et al., 1995; Hawker et al., 1995; Liu et al., 1999).

Herein, we demonstrate the successful introduction of polarity reversal ketyl strategy to polymer chemistry to realize SCKP. Through this polarity reversal SCKP, the polymerizability of monomers gets reversed, where traditional excellent leaving groups are not suitable for polymerization but challenging polymerizations involving the cleavage of challenging C-F and C-CF₃ bonds are realized under mild Barbier conditions. This new polymerization mode also exhibits intriguing tunable polymerization-induced emission properties by simply adjusting monomer structure and polymerization time. This work therefore enables the polymer chemistry with polarity reversal ketyl mode with reversed polymerizability and opens up a reversed and feasible strategy for the polymerization of challenging monomers, which might inspire new reaction, polymerization, and luminescent polymer design.

RESULTS AND DISCUSSION

To demonstrate the above hypothesis of reductive polarity reversal mechanism, the reaction between fluorobenzene and carbonyl compounds was carried out under Barbier conditions, where the reaction exhibits reversed reactivity. The reactivity order of aromatic halides in the polarity reversal ketyl mechanism is C-F > C-Cl (Figure S1 and Tables S1–S3), whereas the conventional reactivity order of aromatic halides is C-Cl >> C-F. Such reaction involving Mg and fluorobenzene is thought of as sluggish, and this result therefore confirms the significance of polarity reversal ketyl mechanism and is therefore of significant importance in organic chemistry. To further confirm the hypothesis of SCKP by introducing polarity reversal ketyl strategy into polymer chemistry, the polymerization of 4-fluorobenzophenone as monomer was carried out in the presence of Mg (1.2 eq.) and 1, 2-dibromoethane (0.2 eq.) at 45°C in THF for 24 h (Figure 4 entry 1). As shown in Figure 2A, the C-F bond is a dormant bond before polarity reversal of reactive C=O bond. After reductive polarity reversal of C=O bond in the formation of ketyl, followed by ER, the dormant C-F bond becomes reactive bond. The activation-cleavage of challenging C-F bond is therefore realized in the polarity reversal strategy, which further enables the SCKP of challenging monomer containing C-F bond.

From the characterizations of the products shown in Figures 2 and S3, the successful formation of polymer can be verified obviously from the comparison of NMR spectra, where sharp ^1H NMR signals of monomer disappear and broader aromatic and hydroxide signals of polymer appear at 7.60–6.75 and 3.83–3.35 ppm, respectively. From comparison of the ^{13}C NMR spectra of the monomer and the polymer, the carbonyl

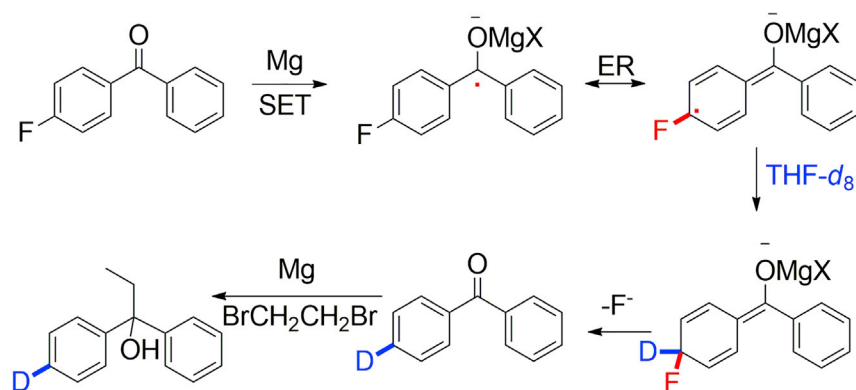


Figure 3. Validation of the Self-Condensing Ketyl Polymerization Mechanism via a Deuterium Labeling Experiment

signal at 195.33 ppm can be seen to disappear and the fluorobenzene signals at 166.67 and 164.15 ppm decrease, which confirms that the polymer contains fluorobenzene as an end group. The existence of this fluorobenzene end group is confirmed by ^{19}F NMR signal at 115.46 ppm. The successful formation of the polymer is further verified by gel permeation chromatography (GPC) characterization with a M_n of 3,400 g/mol and \bar{D} of 1.40. The chemical structure of the polymer is further verified by the Fourier transform infrared (FTIR) spectrum, which contains groups like C-OH, phenyl, and fluorobenzene. The characteristic glass transition temperature (T_g) of fluoro-poly(triphenylmethanol) (fluoro-PTPM) was measured by differential scanning calorimetry (DSC) with a T_g of $\sim 104.7^\circ\text{C}$ (Figure S3).

To confirm the polymerization mechanism, matrix-assisted laser desorption ionization time-of-flight (MALDI-TOF) mass spectrometry was utilized to characterize the polymer sample obtained after 10 min of polymerization, as shown in Figures 2D–2F and S4. From the complete spectrum, an m/z difference of 182.196 can be clearly observed as the molecular weight of the repeating unit, which is consistent with the molecular weight of diphenylmethanol group (182.073 Da). From the enlarged spectrum of pentamer, every peak can be identified and assigned as [M]-3OH, [M]-2OH, [M]-OH-nH, [M], and [M]+ Na^+ . The chemical structure of fluoro-PTPM is further supported by comparison of the similarity between the observed and calculated isotope peaks of [M], [M]-OH-nH, and [M]-2OH, signals that show a very similar isotope pattern. All these results confirm the hypothesized polarity reversal SCKP mechanism shown in Figures 1B and 2A, which relies on the polarity reversal of reactive ketone group in the formation of ketyl intermediates and ER triggered C-F bond activation-cleavage, resulting in polymerization through further SCKP.

To further confirm the above polymerization mechanism, a deuterium labeling experiment was carried out in THF-d_8 with 3 eq. of Mg and 1 eq. of 1, 2-dibromoethane at 45°C . The greatly increased amounts of Mg and 1, 2-dibromoethane will influence the reductive polarity reversal process via SET and interrupt the polymerization process, so that the intermediate should be captured. Through the deuterium labeling experiment, *para*-deuterated diphenylethylmethanol with 6% isolated yield and 35% deuterated ratio was successfully captured (Figure 3 and Figures S28–S32). According to the analysis shown in Figure 3, the only possible pathway to the formation of *para*-deuterated diphenylethylmethanol requires the reductive polarity reversal of carbonyl via a SET in the formation of a ketyl radical anion intermediate, the C-F activation via ER of the ketyl radical anion intermediate, the hydrogen/deuterium abstraction reaction between the ER ketyl radical anion intermediate and THF-d_8 as found in the literature (Clerici et al., 2005; Pryor et al., 1983), the C-F cleavage via ER in the formation of carbonyl compound, and the addition of the Grignard reagent. To further clarify the polymerization process of SCKP through polarity reversal ketyl mechanism, ^1H NMR and FTIR techniques were carried out with different substituents as leaving groups (Figures S8–S12 and 4A). The failure of polymerization of AB-type dimer containing both C-F and C=O moieties indicates the importance of C-F activation-cleavage triggered by ER in SCKP (Figure 4A entry 2). This also indicates that the polymerization mechanism of SCKP is not a traditional AB-type polycondensation, which is further confirmed by controlled experiments of polymerization of AB-type bifunctional 4-fluorobenzophenone in the presence of 1 eq. of monofunctional fluorobenzene or benzophenone. In this nontraditional AB-type polycondensation, monofunctional fluorobenzene did not inhibit the polymerization but monofunctional benzophenone did (Figure 4A entries 3 and 4). The

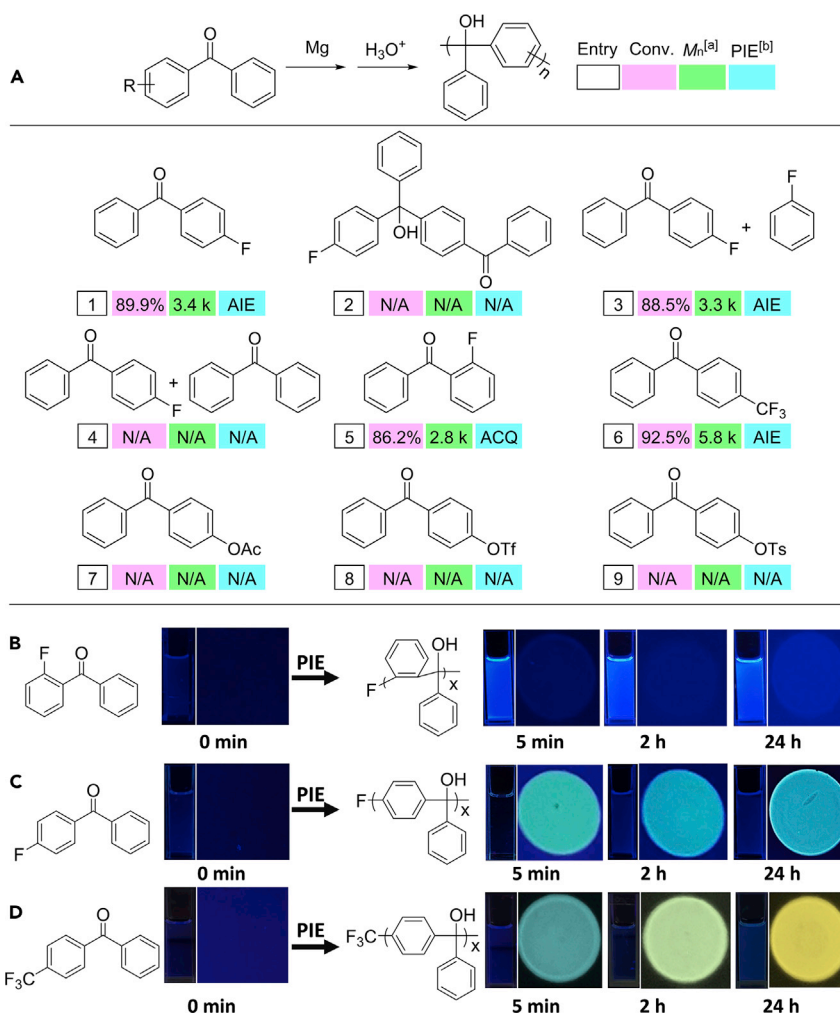


Figure 4. Results of Self-Condensing Ketyl Polymerization

Reaction conditions: monomer (1.0 g, 1.0 eq.), Mg (1.2 eq.), 1, 2-dibromoethane (0.2 eq.), THF (10 mL), 45°C, 24 h;

^[a]measured by GPC; ^[b]polymerization-induced emission.

(A) Substrate range of self-condensing ketyl polymerization.

(B) Emission digital photos of polymerization process of 2-fluorobenzophenone at different polymerization times (under irradiation with UV lamp at 365 nm).

(C) Emission digital photos of polymerization process of 4-fluorobenzophenone at different polymerization times (under irradiation with UV lamp at 365 nm).

(D) Emission digital photos of polymerization process of 4-trifluoromethylbenzophenone at different polymerization times (under irradiation with UV lamp at 365 nm).

evidences of obvious polymer signal observed at 15 min with conversion as low as 28.8%, successful isolation of 3.2% yield of dimer (d) after 24 h of polymerization, and still more than 10% of monomer observed after 24 h of polymerization also confirm this SCKP is not a traditional AB-type polycondensation (Figures S5 and S6). FTIR tracing experiments verify that this SCKP process contains carbonyl addition process and C-F activation-cleavage process with decreased carbonyl signal, increased C-O signal, and decreased fluorophenyl signal (Figure S6).

These above results therefore confirm the proposed polymerization mechanism shown in Figure 1B. In the reductive polarity reversal mechanism, carbonyl addition happens first via a SET between carbonyl and Mg in the formation of ketyl. C-F activation happens second via ER of ketyl and, third, is followed by a coupling reaction between (b) and (b*) to initiate the polymerization of (b*). The fourth step is the C-F cleavage via ER in the formation of the carbonyl end group, which will further react with Mg via SET to

complete chain propagation with one monomer inserted. Attributed to the continuous relay of reactions in the order of carbonyl addition via SET in the formation of ketyl, C-F activation via ER, and ketyl coupling and C-F cleavage via ER, the SCKP is realized through polarity reversal ketyl mechanism. This polarity reversal ketyl mechanism exhibits intriguing reversed polymerizability as well. With traditional leaving groups like acetoxo (OAc), tosylate (OTs), and triflate (OTf), which could react with Mg directly, their failures in polymerization indicate that the direct activation-cleavage of leaving groups by Mg would interrupt SCKP (Figure 4A entry 7–9). However, with even more challenging trifluoromethyl (CF₃) substituent as leaving group, its SCKP is realized successfully (Figure 4A entry 6). These results indicate that polarity reversal strategy of SCKP enables the polymerization of challenging monomers through activation-cleavage of challenging bonds under mild conditions. It is worth mentioning that this discovery might open up a reversed and feasible strategy for the polymerization of challenging monomers, which might further inspire new reaction and polymerization.

Photophysical properties are intriguing phenomena with potential optical, electronic, and sensory applications (Lv et al., 2017, 2019; Wan et al., 2017, 2018). To illustrate the advantage of this SCKP, photophysical properties of the obtained PTPMs and the polymerization process were investigated (Figures 4B–4D and S13–S16). From the results, these PTPMs exhibit obviously site-specific luminescence that can be simply adjusted by monomer structures. When the phenyl rings of obtained *para*-PTPMs are rotation free, they are aggregation-induced emission (AIE)-type luminescence, similar to Tang's reports (Hong et al., 2011; Liu et al., 2020; Luo et al., 2001; Mei et al., 2015; Zhang et al., 2017). When the rotation about the phenyl rings is hindered, the *ortho*-PTPM exhibits traditional luminescence with aggregation caused quenching (ACQ) effect. These results confirm that PTPM is a special type of luminescent polymer deriving from the intramolecular and intermolecular through-space conjugation effect under polymer chain constraint and intramolecular charge-transfer effect (Jing et al., 2019; Sun et al., 2017). Interestingly, the terminal groups of PTPMs are significant to their luminescence. When the terminal group is a fluoro group, *para*-PTPM is AIE with cyan color, whereas that of trifluoromethyl group is AIE with yellow color. Time-dependent density functional theory calculations indicate terminal groups have significant influences on the band gaps and dihedral angles, which further cause the differences on luminescence (Figures S17 and S18). The band gaps of both F-PTPM and CF₃-PTPM decrease with the increase of chain length, which indicates the through-space conjugation under polymer chain constraint plays important roles in the luminescent properties. Besides, obviously different HOMO, LUMO, and band gaps are observed between F-PTPMs and CF₃-PTPMs with different chain lengths, causing the differences in luminescent properties of PTPMs with different terminal groups. SCKP also exhibits polymerization-induced emission property, which can be tuned from ACQ type to AIE type by simply adjusting monomer structures (Figures 4B–4D). The luminescence color of AIE-type polymerization-induced emission can be tuned as well from cyan to yellow by simply adjusting monomer structures and polymerization time. This tunable polymerization-induced emission is due to the formation of luminescent non-conjugated PTPM during polymerization. In comparison, luminescent polymers are generally designed by polymerization of luminescent monomers, where polymerization has a limited effect on the design of luminescent polymers. This result therefore opens up a new avenue to design luminescent polymers through polymerization of nonemissive monomers *in situ*.

Conclusion

In conclusion, the successful introduction of polarity reversal ketyl strategy into polymer chemistry has been realized through SCKP. In this polarity reversal approach, it exhibits intriguing reversed polymerizability, where traditional excellent leaving groups are not suitable for polymerization but challenging polymerizations involving the cleavage of C-F and C-CF₃ bonds are realized under mild Barbier conditions. The SCKP involves continuous relay of reactions in the order of carbonyl addition via SET in the formation of ketyl intermediate, C-F activation via ER, and ketyl coupling and C-F cleavage via ER in one polymerization cycle. This SCKP also exhibits intriguing polymerization-induced emission capability to construct luminescent polymers from nonemissive monomers and the emissive properties vary from traditional luminescence to AIE-type luminescence with emission color varying from blue to cyan and yellow, which can be simply adjusted by adjusting the monomer structure and polymerization time. This work therefore provides polymer chemistry with polarity reversal ketyl strategy and opens up a new avenue toward the polymerization of challenging C-X bonds, which might inspire new reaction, polymerization, and luminescent polymer design.

Limitations of the Study

This study focuses on the demonstration of the introduction of polarity reversal strategy into polymer chemistry to demonstrate the advantage of resplendent polarity reversal mechanism with reversed polymerizability. The substrates used in this study limit on carbonyl compounds, and further investigations on other groups will expand the utilization of this polymerization methodology. Fortunately, carbonyl compounds account for a high portion in organic chemicals and have played significant cornerstone roles in organic chemistry, which might expand the monomer library of polymer materials and inspire the design of novel polymer from carbonyl chemicals.

METHODS

All methods can be found in the accompanying [Transparent Methods supplemental file](#).

SUPPLEMENTAL INFORMATION

Supplemental Information can be found online at <https://doi.org/10.1016/j.isci.2020.101031>.

ACKNOWLEDGMENTS

We acknowledge funding support from NSFC (21971236, 21922112, 21672213 and 21871258), the National Key R&D Program of China (Grant No. 2017YFA0700103), and the Haixi Institute of CAS (Grant No. CXZX-2017-P01). This work is dedicated to Professor Cai-Yuan Pan, University of Science and Technology of China, for his 80th birthday in May 2020.

AUTHOR CONTRIBUTIONS

S.-S.L. performed the polymerization experiments and analyzed the data. N.Z. performed the organic chemistry experiments and analyzed the data. Y.-N.J. assisted on polymerization and performed calculations. W.-M.W. conceived the concept. Y.L., H.B., and W.-M.W. designed the study and wrote the manuscript.

DECLARATION OF INTERESTS

The authors declare no competing interests.

Received: February 8, 2020

Revised: March 25, 2020

Accepted: March 29, 2020

Published: April 24, 2020

REFERENCES

- Ahrens, T., Kohlmann, J., Ahrens, M., and Braun, T. (2015). Functionalization of fluorinated molecules by transition-metal-mediated C-F bond activation to access fluorinated building blocks. *Chem. Rev.* *115*, 931–972.
- Amii, H., and Uneyama, K. (2009). C-F bond activation in organic synthesis. *Chem. Rev.* *109*, 2119–2183.
- Baggett, A.W., Guo, F., Li, B., Liu, S.Y., and Jäkle, F. (2015). Regioregular synthesis of Azaborine oligomers and a polymer with a syn Conformation stabilized by NH $\cdots\pi$ interactions. *Angew. Chem. Int. Ed.* *54*, 11191–11195.
- Bao, Z., Chan, W.K., and Yu, L. (1995). Exploration of the Stille coupling reaction for the synthesis of functional polymers. *J. Am. Chem. Soc.* *117*, 12426–12435.
- Berger, A.L., Donabauer, K., and König, B. (2018). Photocatalytic Barbier reaction - visible-light induced allylation and benzylation of aldehydes and ketones. *Chem. Sci.* *9*, 7230–7235.
- Bielawski, C.W., and Grubbs, R.H. (2000). Highly efficient ring-opening metathesis polymerization (ROMP) using new ruthenium catalysts containing N-heterocyclic carbene ligands. *Angew. Chem. Int. Ed.* *39*, 2903–2906.
- Bielawski, C.W., and Grubbs, R.H. (2007). Living ring-opening metathesis polymerization. *Prog. Polym. Sci.* *32*, 1–29.
- Blomberg, C. (1993). *The Barbier Reaction and Related One-step Processes* (Springer-Verlag).
- Blomberg, C., and Hartog, F.A. (1977). Barbier reaction - one-step alternative for syntheses via organomagnesium compounds. *Synthesis* (Stuttg.), 18–30.
- Chiefari, J., Chong, Y.K., Ercole, F., Krstina, J., Jeffery, J., Le, T.P.T., Mayadunne, R.T.A., Meijs, G.F., Moad, C.L., Moad, G., et al. (1998). Living free-radical polymerization by reversible addition-fragmentation chain Transfer: the RAFT process. *Macromolecules* *31*, 5559–5562.
- Clerici, A., Cannella, R., Panzeri, W., Pastori, N., Regolini, E., and Porta, O. (2005). TiCl₃/PhN₂⁺-mediated radical addition of ethers to aldimines generated in situ under aqueous conditions. *Tetrahedron Lett.* *46*, 8351–8354.
- Cui, B.Q., Jia, S.C., Tokunaga, E., and Shibata, N. (2018). Defluorosilylation of fluoroarenes and fluoroalkanes. *Nat. Commun.* *9*, 4393.
- Deng, X.X., Li, L., Li, Z.L., Lv, A., Du, F.S., and Li, Z.C. (2012). Sequence regulated poly(ester-amide)s based on Passerini reaction. *ACS Macro Lett.* *1*, 1300–1303.
- Deng, H.Q., Han, T., Zhao, E.G., Kwok, R.T.K., Lam, J.W.Y., and Tang, B.Z. (2016). Multicomponent click polymerization: a facile strategy toward fused heterocyclic polymers. *Macromolecules* *49*, 5475–5483.
- Fréchet, J.M.J., Henmi, M., Gitsov, I., Aoshima, S., Leduc, M.R., and Grubbs, R.B. (1995). Self-condensing vinyl polymerization - an approach to dendritic materials. *Science* *269*, 1080–1083.

- Guo, F., Yin, X., Pammer, F., Cheng, F., Fernandez, D., Lalancette, R.A., and Jäkle, F. (2014). Regioregular organoborane-functionalized poly(3-alkynylthiophene)s. *Macromolecules* 47, 7831–7841.
- Hart, D.J. (1984). Free-radical carbon-carbon bond formation in organic synthesis. *Science* 223, 883–887.
- Hawker, C.J., Frechet, J.M.J., Grubbs, R.B., and Dao, J. (1995). Preparation of hyperbranched and star polymers by a "living", self-condensing free radical polymerization. *J. Am. Chem. Soc.* 117, 10763–10764.
- Hawker, C.J., and Wooley, K.L. (2005). The convergence of synthetic organic and polymer chemistries. *Science* 309, 1200–1205.
- He, B.Z., Zhen, S.J., Wu, Y.W., Hu, R.R., Zhao, Z.J., Qin, A.J., and Tang, B.Z. (2016). Cu(I)-Catalyzed amino-yne click polymerization. *Polym. Chem.* 7, 7375–7382.
- He, B.Z., Su, H.F., Bai, T.W., Wu, Y.W., Li, S.W., Gao, M., Hu, R.R., Zhao, Z.J., Qin, A.J., Ling, J., et al. (2017). Spontaneous amino-yne click polymerization: a powerful tool toward regio- and stereospecific poly(beta-aminoacrylate)s. *J. Am. Chem. Soc.* 139, 5437–5443.
- Hong, C.Y., You, Y.Z., Wu, D.C., Liu, Y., and Pan, C.Y. (2007). Thermal control over the topology of cleavable polymers: from linear to hyperbranched structures. *J. Am. Chem. Soc.* 129, 5354–5355.
- Hong, Y., Lam, J.W.Y., and Tang, B.Z. (2011). Aggregation-induced emission. *Chem. Soc. Rev.* 40, 5361–5388.
- Huang, H., Wang, W., Zhou, Z., Sun, B., An, M., Haefner, F., and Niu, J. (2019). Radical ring-closing/ring-opening cascade polymerization. *J. Am. Chem. Soc.* 141, 12493–12497.
- Iha, R.K., Wooley, K.L., Nystrom, A.M., Burke, D.J., Kade, M.J., and Hawker, C.J. (2009). Applications of orthogonal "click" chemistries in the synthesis of functional soft materials. *Chem. Rev.* 109, 5620–5686.
- Jiang, K.M., Zhang, L., Zhao, Y.C., Lin, J., and Chen, M. (2018). Palladium-Catalyzed cross-coupling polymerization: a new access to cross-conjugated polymers with modifiable structure and tunable optical/conductive properties. *Macromolecules* 51, 9662–9668.
- Jing, Y.N., Li, S.S., Su, M., Bao, H., and Wan, W.M. (2019). Barbier hyperbranching polymerization-induced emission toward facile fabrication of white LED and light harvesting film. *J. Am. Chem. Soc.* 141, 16839–16848.
- Kotha, S., Lahiri, K., and Kashinath, D. (2002). Recent applications of the Suzuki–Miyaura cross-coupling reaction in organic synthesis. *Tetrahedron* 58, 9633–9695.
- Kreye, O., Toth, T., and Meier, M.A.R. (2011). Introducing multicomponent reactions to polymer science: Passerini reactions of renewable monomers. *J. Am. Chem. Soc.* 133, 1790–1792.
- Li, C.J., and Zhang, W.C. (1998). Unexpected Barbier–Grignard allylation of aldehydes with magnesium in water. *J. Am. Chem. Soc.* 120, 9102–9103.
- Littke, A.F., Dai, C., and Fu, G.C. (2000). Versatile catalysts for the Suzuki cross-coupling of arylboronic acids with aryl and vinyl halides and triflates under mild conditions. *J. Am. Chem. Soc.* 122, 4020–4028.
- Littke, A.F., and Fu, G.C. (1999). The first general method for Stille cross-couplings of aryl chlorides. *Angew. Chem. Int. Ed.* 38, 2411–2413.
- Liu, B., Zhang, H., Liu, S., Sun, J., Zhang, X., and Tang, B.Z. (2020). Polymerization-induced emission. *Mater. Horiz.* <https://doi.org/10.1039/c1039mh01909j>.
- Liu, M., Vladimirov, N., and Fréchet, J.M.J. (1999). A new approach to hyperbranched polymers by ring-opening polymerization of an AB monomer: 4-(2-Hydroxyethyl)-epsilon-caprolactone. *Macromolecules* 32, 6881–6884.
- Liu, Y., Wu, D.C., Ma, Y.X., Tang, G.P., Wang, S., He, C.B., Chung, T.S., and Goh, S. (2003). Novel poly(amino ester)s obtained from Michael addition polymerizations of trifunctional amine monomers with diacrylates: safe and efficient DNA carriers. *Chem. Commun.* 2630–2631.
- Luo, J.D., Xie, Z.L., Lam, J.W.Y., Cheng, L., Chen, H.Y., Qiu, C.F., Kwok, H.S., Zhan, X.W., Liu, Y.Q., Zhu, D.B., et al. (2001). Aggregation-induced emission of 1-methyl-1,2,3,4,5-pentaphenylsilole. *Chem. Commun.* 1740–1741.
- Lv, X.H., Li, S.S., Tian, C.Y., Yang, M.M., Li, C., Zhou, Y., Sun, X.L., Zhang, J., and Wan, W.M. (2017). Borinic acid polymer: simplified synthesis and enzymatic biofuel cell application. *Macromolecular Rapid Commun.* 38, 1600687.
- Lv, X.H., Wang, X.Y., Zhou, Y., Xu, H., and Wan, W.M. (2019). Promoting water dissociation performance by borinic acid for the strong-acid/base-free hydrogen evolution reaction. *Chem. Commun.* 55, 9821–9824.
- Mei, J., Leung, N.L.C., Kwok, R.T.K., Lam, J.W.Y., and Tang, B.Z. (2015). Aggregation-induced emission: together we shine, united we soar! *Chem. Rev.* 115, 11718–11940.
- Meissner, G., Kretschmar, K., Braun, T., and Kemnitz, E. (2017). Consecutive transformations of tetrafluoropropenes: hydrogermylation and catalytic C-F activation steps at a Lewis acidic aluminum fluoride. *Angew. Chem. Int. Ed.* 56, 16338–16341.
- Miyaura, N., Yanagi, T., and Suzuki, A. (1981). The palladium-catalyzed cross-coupling reaction of phenylboronic acid with haloarenes in the presence of bases. *Synth. Commun.* 11, 513–519.
- Moad, G., Rizzardo, E., and Thang, S.H. (2008). Radical addition–fragmentation chemistry in polymer synthesis. *Polymer* 49, 1079–1131.
- Pintauer, T., and Matyjaszewski, K. (2008). Atom transfer radical addition and polymerization reactions catalyzed by ppm amounts of copper complexes. *Chem. Soc. Rev.* 37, 1087–1097.
- Pryor, W.A., Ohto, N., and Church, D.F. (1983). Reaction of cumene with ozone to form cumyl hydrotrioxide and the kinetics of decomposition of cumyl hydrotrioxide. *J. Am. Chem. Soc.* 105, 3614–3622.
- Schluter, A.D. (2001). The tenth anniversary of Suzuki polycondensation (SPC). *J. Polym. Sci. A Polym. Chem.* 39, 1533–1556.
- Sergeev, G.B., Smirnov, V.V., and Badaev, F.Z. (1982). Low-temperature reaction of magnesium with fluorobenzene. *J. Organomet. Chem.* 224, C29–C30.
- Song, Y., Ji, X., Dong, M., Li, R., Lin, Y.N., Wang, H., and Wooley, K.L. (2018). Advancing the development of highly-functionalizable glucose-based polycarbonates by tuning of the glass transition temperature. *J. Am. Chem. Soc.* 140, 16053–16057.
- Sun, X.L., Liu, D.M., Tian, D., Zhang, X.Y., Wu, W., and Wan, W.M. (2017). The introduction of the Barbier reaction into polymer chemistry. *Nat. Commun.* 8, 1210.
- Tian, P.P., Feng, C., and Loh, T.P. (2015). Rhodium-catalysed C(sp²)-C(sp²) bond formation via C-H/C-F activation. *Nat. Commun.* 6, 7472.
- Tsao, Y.T., and Wooley, K.L. (2017). Synthetic, functional thymidine-derived polydeoxyribonucleotide analogues from a six-membered cyclic phosphoester. *J. Am. Chem. Soc.* 139, 5467–5473.
- Vougioukalakis, G.C., and Grubbs, R.H. (2010). Ruthenium-based heterocyclic carbene-coordinated olefin metathesis catalysts. *Chem. Rev.* 110, 1746–1787.
- Wan, W.M., Li, S.S., Liu, D.M., Lv, X.H., and Sun, X.L. (2017). Synthesis of electron-deficient borinic acid polymers with multiresponsive properties and their application in the fluorescence detection of alizarin red S and electron-rich 8-hydroxyquinoline and fluoride ion: substituent effects. *Macromolecules* 50, 6872–6879.
- Wan, W.M., Tian, D., Jing, Y.N., Zhang, X.Y., Wu, W., Ren, H., and Bao, H.L. (2018). NBN-doped conjugated polycyclic aromatic hydrocarbons as an AIEgen class for extremely sensitive detection of explosives. *Angew. Chem. Int. Ed.* 57, 15510–15516.
- Wang, J.S., and Matyjaszewski, K. (1995). Controlled/"living" radical polymerization. atom transfer radical polymerization in the presence of transition-metal complexes. *J. Am. Chem. Soc.* 117, 5614–5615.
- Wang, D., Liu, Y., Hu, Z.C., Hong, C.Y., and Pan, C.Y. (2005). Michael addition polymerizations of trifunctional amines with diacrylamides. *Polymer* 46, 3507–3514.
- Wang, H.N., Dai, X.J., and Li, C.J. (2017). Aldehydes as alkyl carbanion equivalents for additions to carbonyl compounds. *Nat. Chem.* 9, 374–378.
- Wang, L., Lear, J.M., Rafferty, S.M., Fosu, S.C., and Nagib, D.A. (2018). Ketyl radical reactivity via atom transfer catalysis. *Science* 362, 225–229.

Wei, B., Li, W.Z., Zhao, Z.J., Qin, A.J., Hu, R.R., and Tang, B.Z. (2017). Metal-free multicomponent tandem polymerizations of alkynes, amines, and formaldehyde toward structure- and sequence-controlled luminescent polyheterocycles. *J. Am. Chem. Soc.* *139*, 5075–5084.

Wu, H.B., Wang, Z.M., and Tao, L. (2017). The Hantzsch reaction in polymer chemistry: synthesis and tentative application. *Polym. Chem.* *8*, 7290–7296.

Xue, H.D., Zhao, Y., Wu, H.B., Wang, Z.L., Yang, B., Wei, Y., Wang, Z.M., and Tao, L. (2016). Multicomponent combinatorial polymerization via the Biginelli reaction. *J. Am. Chem. Soc.* *138*, 8690–8693.

Yin, X., Guo, F., Lalancette, R.A., and Jäkle, F. (2016). Luminescent main-chain organoborane polymers: highly robust, electron-deficient poly(oligothiophene borane)s via Stille coupling polymerization. *Macromolecules* *49*, 537–546.

Yokoyama, A., Suzuki, H., Kubota, Y., Ohuchi, K., Higashimura, H., and Yokozawa, T. (2007). Chain-growth polymerization for the synthesis of polyfluorene via Suzuki-Miyaura coupling reaction from an externally added initiator unit. *J. Am. Chem. Soc.* *129*, 7236–7237.

Zhang, H.K., Zheng, X.Y., Xie, N., He, Z.K., Tiu, J.K., Leung, N.L.C., Niu, Y.L., Huang, X.H., Wong, K.S., Kwok, R.T.K., et al. (2017). Why do simple molecules with "isolated" phenyl rings emit visible light? *J. Am. Chem. Soc.* *139*, 16264–16272.

Zhang, W.C., and Li, C.J. (1999). Magnesium-mediated carbon–carbon bond formation in aqueous media: Barbier–Grignard allylation and pinacol coupling of aldehydes. *J. Org. Chem.* *64*, 3230–3236.

Zhou, F., and Li, C.J. (2014). The Barbier–Grignard-type arylation of aldehydes using unactivated aryl iodides in water. *Nat. Commun.* *5*, 4254.

Zhu, N., Chiou, M.-F., Xiong, H., Su, M., Su, M., Li, Y., Wan, W.-M., and Bao, H. (2020). The introduction of the radical cascade reaction into polymer chemistry: a one-step strategy for synchronized polymerization and modification. *iScience* *23*, 100902.

iScience, Volume 23

Supplemental Information

Barbier Self-Condensing Ketyl

Polymerization-Induced Emission: A Polarity Reversal Approach to Reversed Polymerizability

Shun-Shun Li, Nengbo Zhu, Ya-Nan Jing, Yajun Li, Hongli Bao, and Wen-Ming Wan

Supplemental Figures

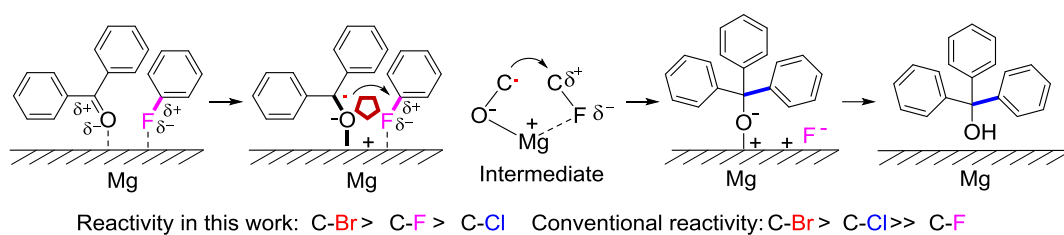


Figure S1. Reductive polarity reversal ketyl mechanism of Mg-mediated C-F bond activation-cleavage, related to **Figure 1**.

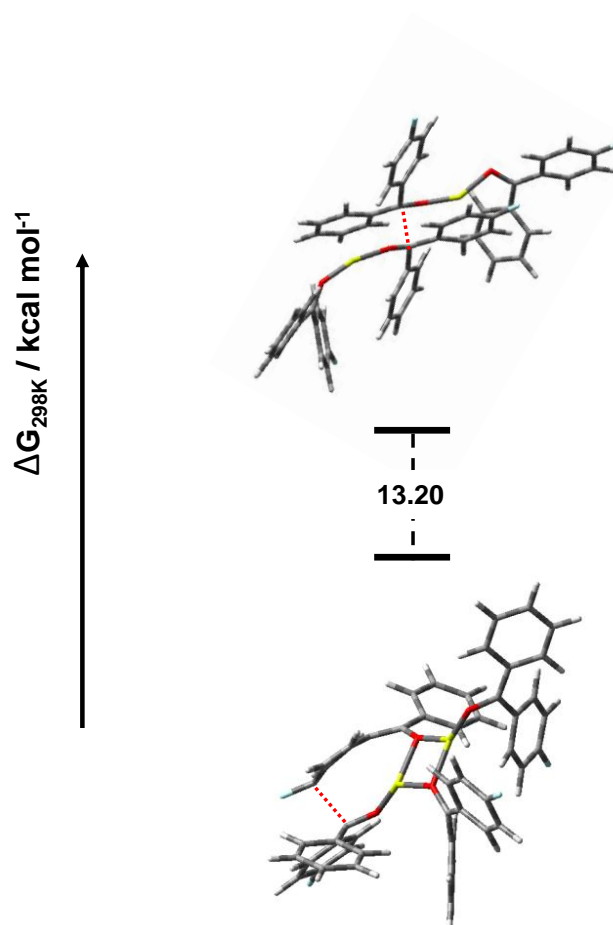


Figure S2. Gibbs free energy profile for the pinacol coupling reaction pathway and radical coupling reaction pathway via electron resonance. Relative free energies are in kcal/mol, related to **Figure 1**.

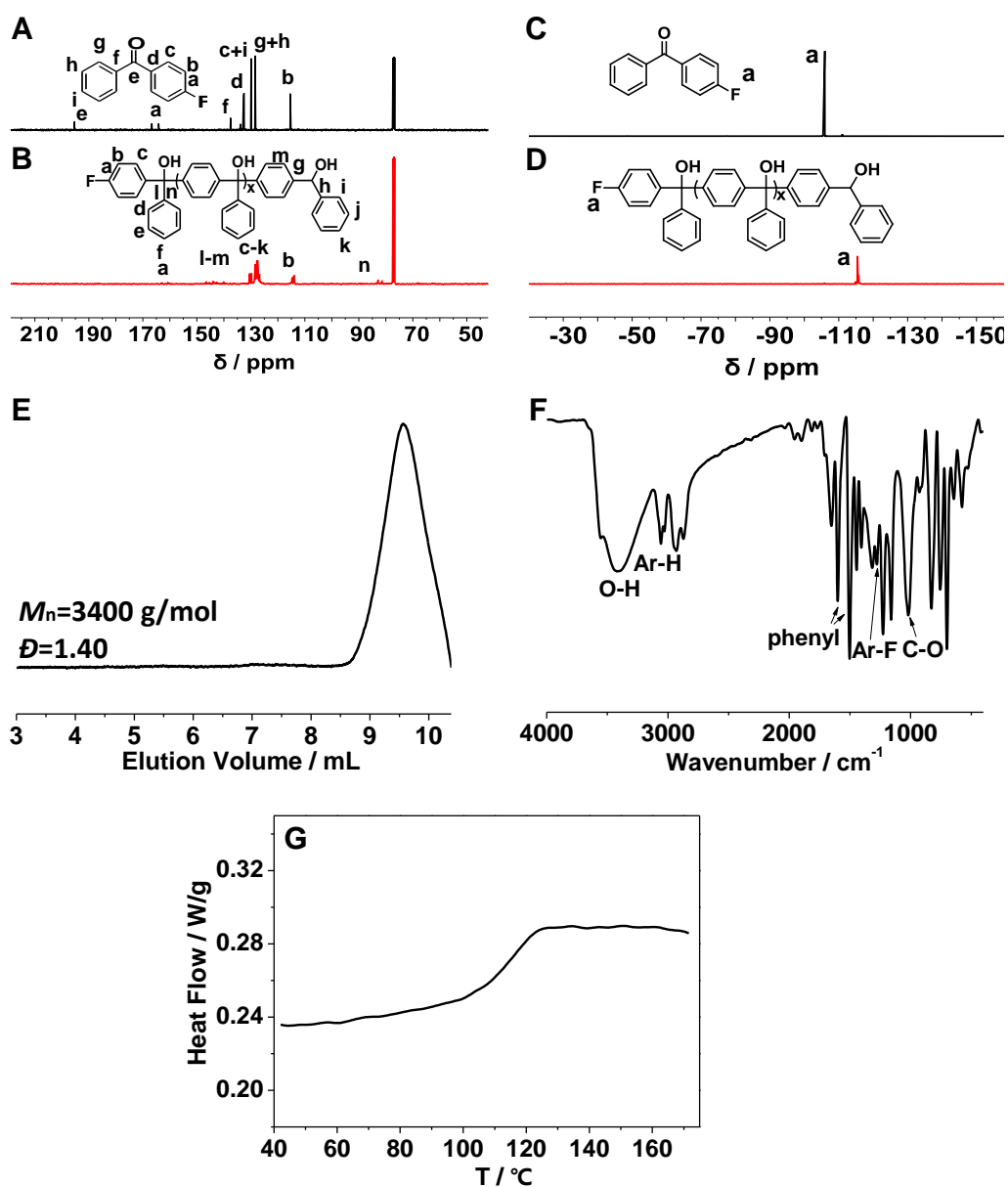


Figure S3. ^{13}C NMR spectra of 4-fluorobenzophenone (A) and fluoro-PTPM (B) in CDCl_3 , ^{19}F NMR spectra of 4-fluorobenzophenone (C) and fluoro-PTPM (D) in CDCl_3 , GPC curve (E), FT-IR spectrum (F) and DSC curve (G) of fluoro-PTPM ($T_g \sim 104.7^\circ\text{C}$), related to **Figure 2**.

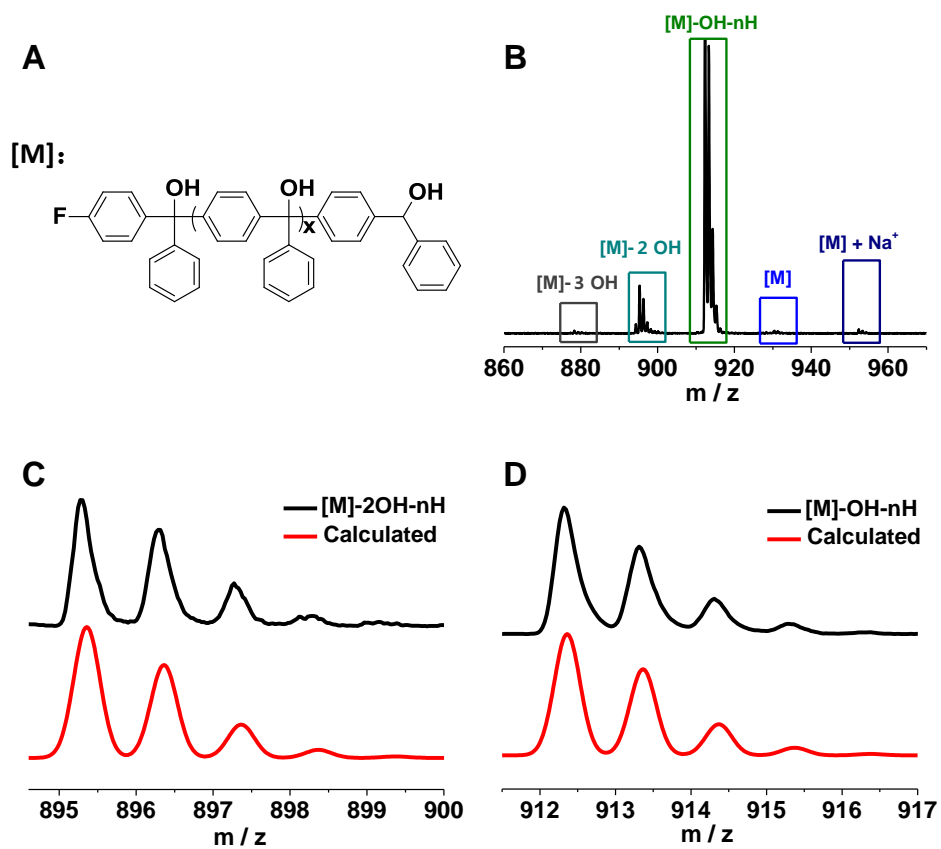


Figure S4. MALDI-TOF characterization of fluoro-PTPM. Chemical structure of fluoro-PTPM (A), enlarged MALDI-TOF spectrum of pentamer (B), comparison of [M]-2OH-nH (DP=5) between observed and calculated spectra (C), comparison of [M]-OH-nH (DP=5) between observed and calculated spectra (D), related to **Figure 2**.

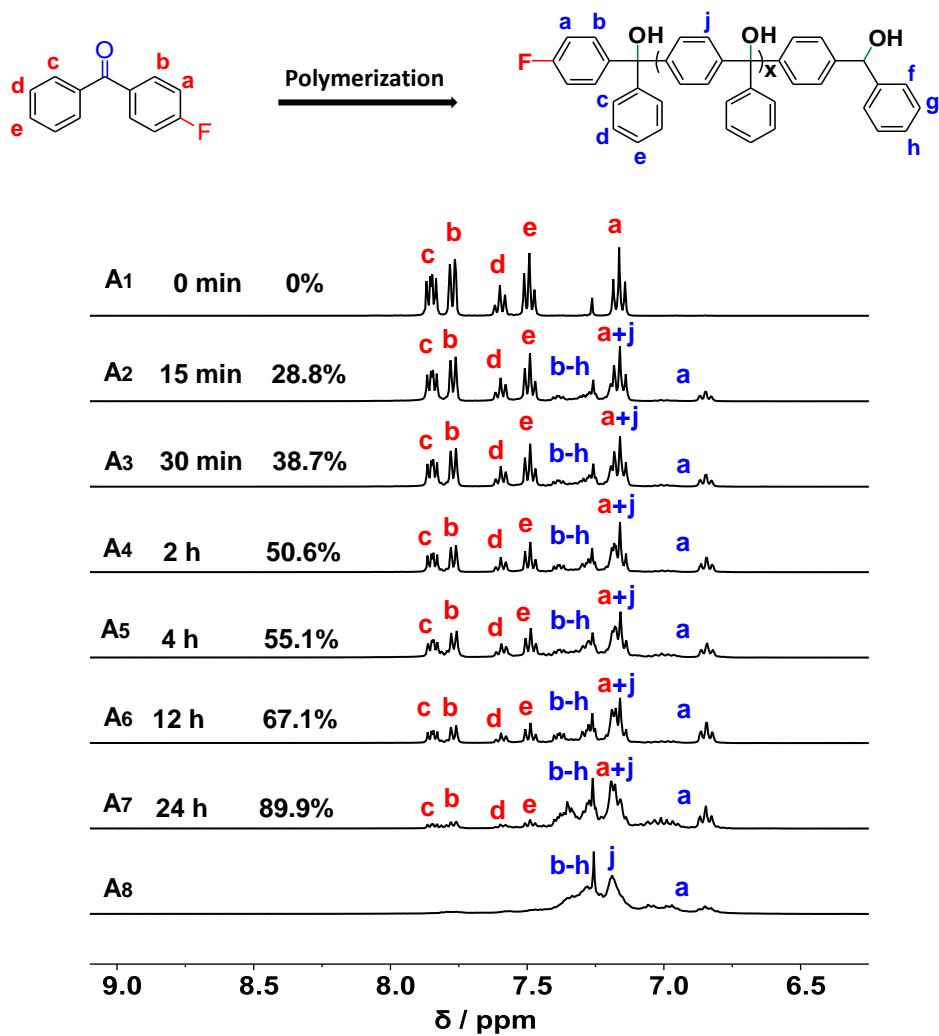


Figure S5. Polymerization process traced by ^1H NMR spectra: monomer (A1), 15min (A2), 30min (A3), 2h (A4), 4h (A5), 12h (A6), 24h (A7) and after precipitation (A8), related to **Figure 2**.

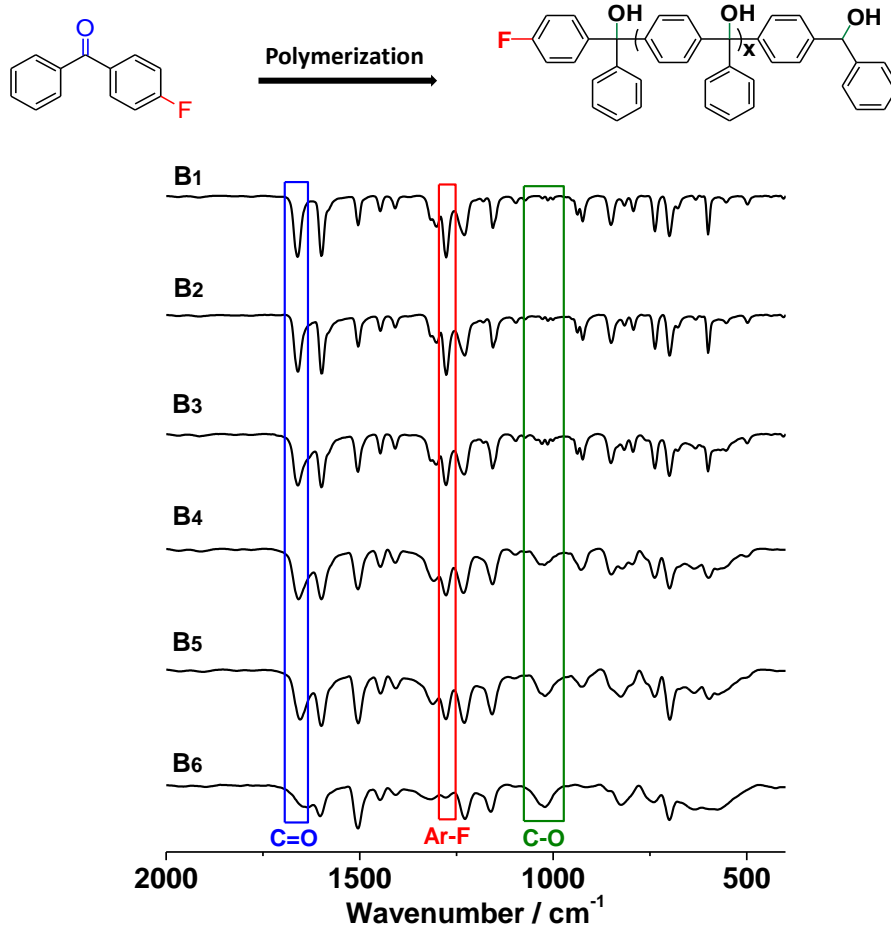


Figure S6. Polymerization process traced by FT-IR spectra: 15min (B1), 30min (B2), 2h (B3), 4h (B4), 12h (B5), 24h (B6), related to **Figure 2**.

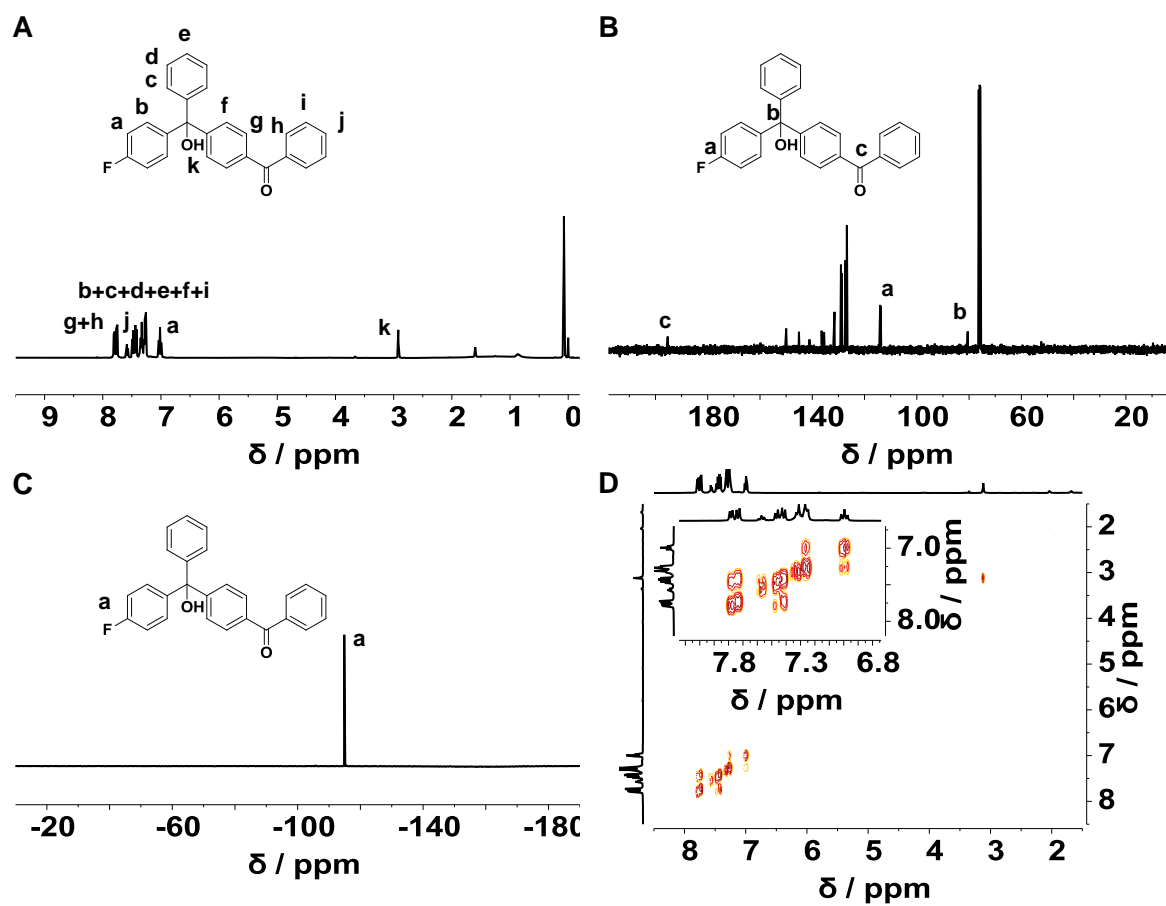


Figure S7. Structural characterizations of isolated dimer intermediate: ^1H NMR spectrum (A), ^{13}C NMR spectrum (B), ^{19}F NMR spectrum and ^1H - ^1H COSY NMR spectrum (D), related to **Figure 4**.

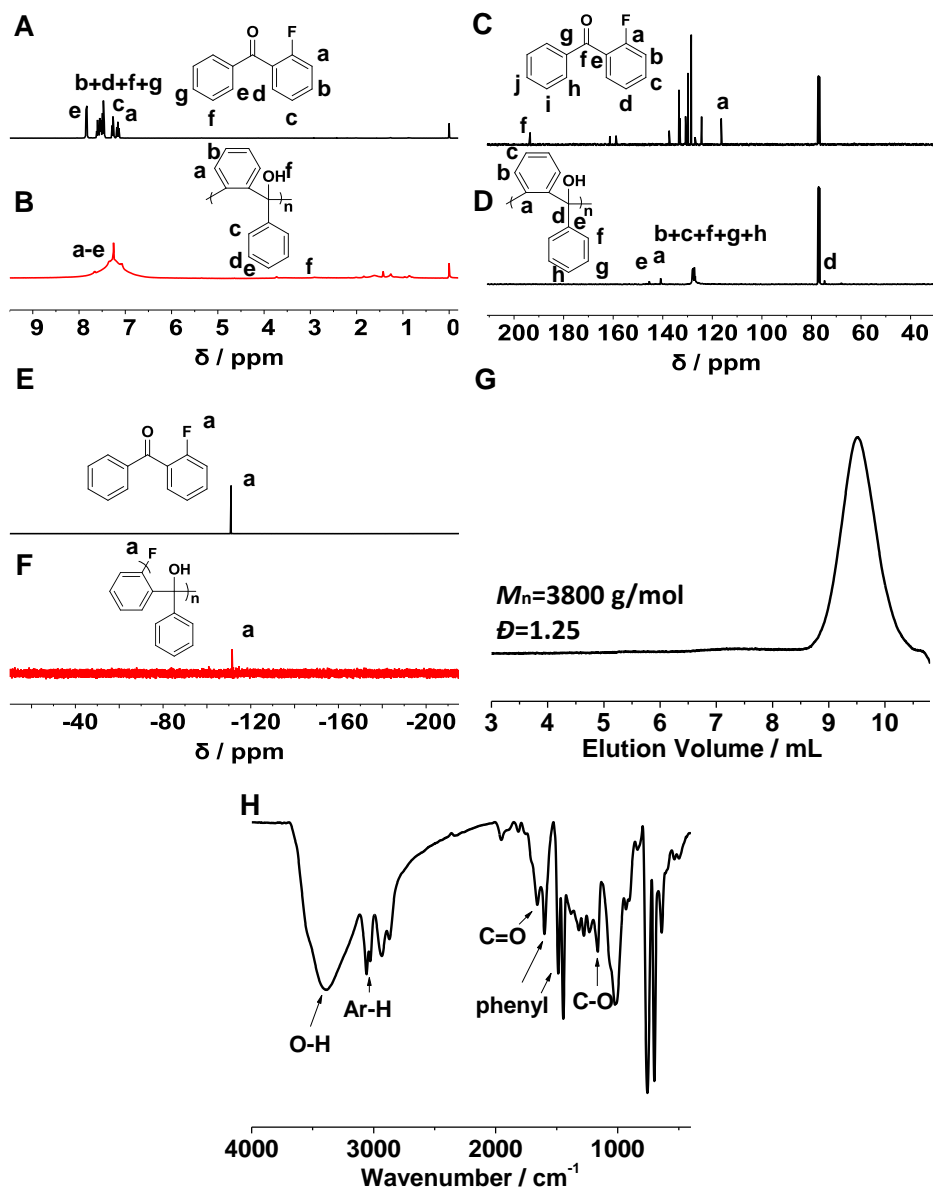


Figure S8. Structural characterization of 2-fluoro-PTPM: ^1H NMR spectra of 2-fluorobenzophenone (A) and 2-fluoro-PTPM (B) in CDCl_3 , ^{13}C NMR spectra of 2-fluorobenzophenone (C) and 2-fluoro-PTPM (D) in CDCl_3 , ^{19}F NMR spectra of 2-fluorobenzophenone (E) and 2-fluoro-PTPM (F) in CDCl_3 , GPC curve (G) and FT-IR spectrum (H) of 2-fluoro-PTPM, related to **Figure 4**.

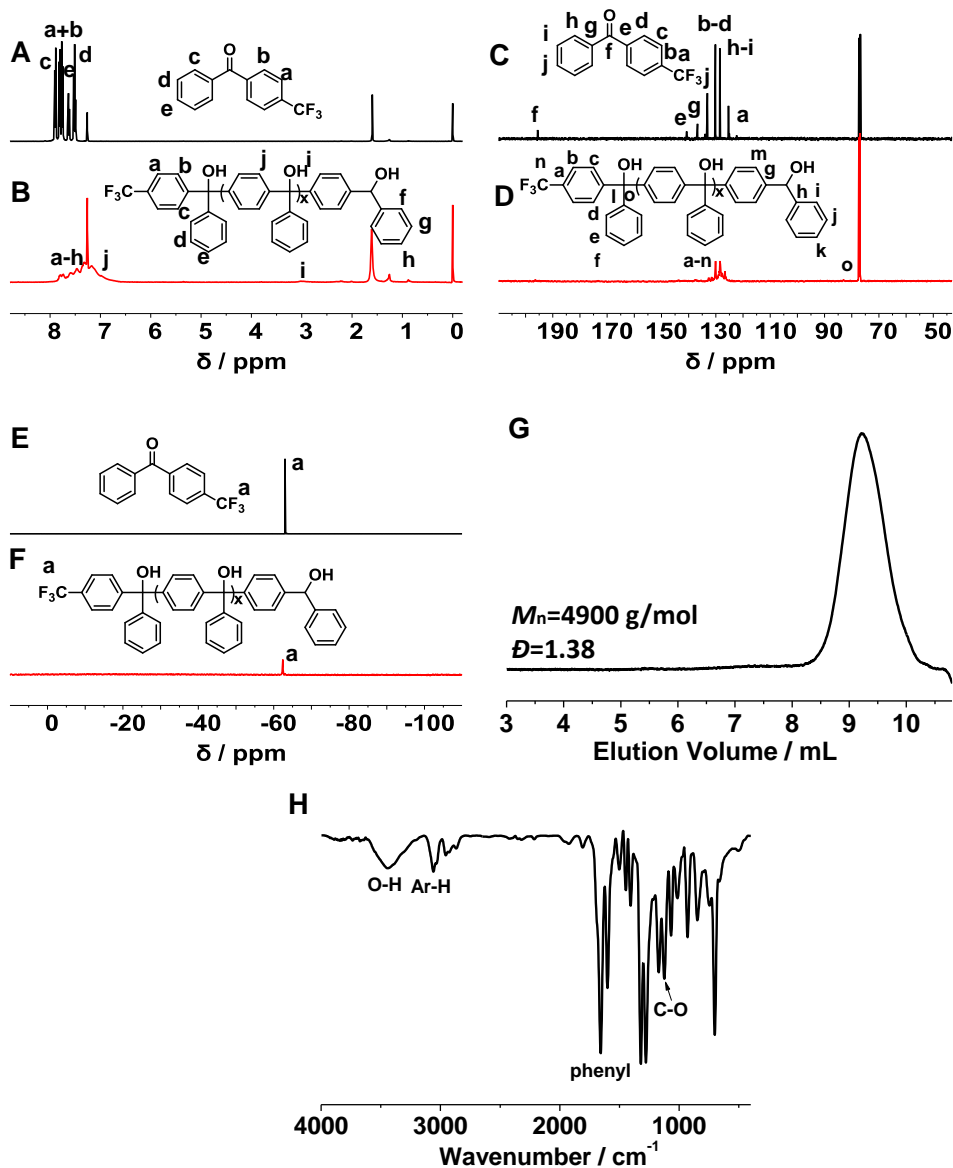


Figure S9. Structural characterization of CF_3 -PTPM: ^1H NMR spectra of 4-trifluoromethylbenzophenone (A) and CF_3 -PTPM (B) in CDCl_3 , ^{13}C NMR spectra of 4-trifluoromethylbenzophenone (C) and CF_3 -PTPM (D) in CDCl_3 , ^{19}F NMR spectra of 4-trifluoromethylbenzophenone (E) and CF_3 -PTPM (F) in CDCl_3 , GPC curve (G) and FT-IR spectrum (H) of CF_3 -PTPM, related to **Figure 4**.

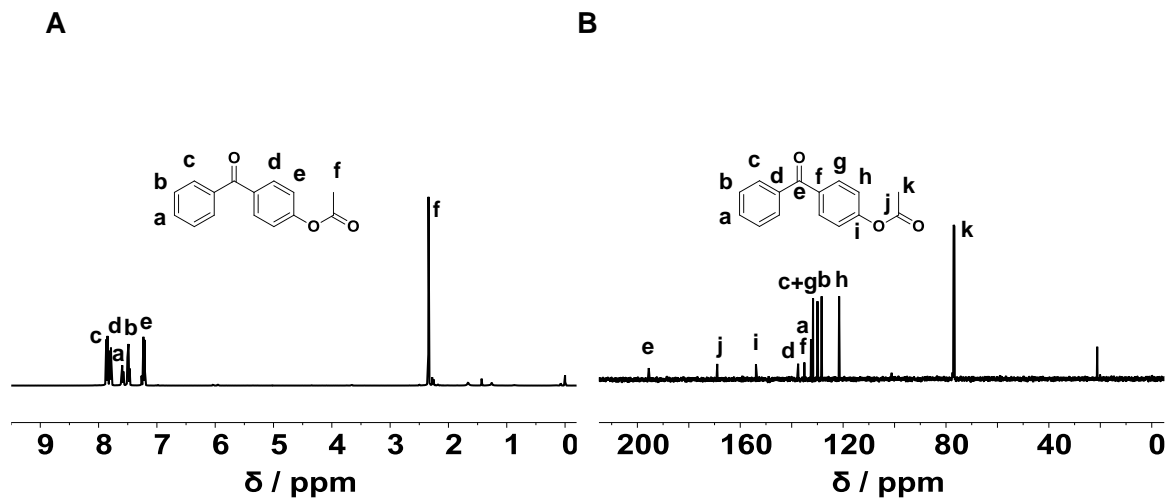


Figure S10. Structural characterization of 4-acetoxybenzophenone: ^1H NMR spectrum (A) and ^{13}C NMR spectrum (B), related to **Figure 4**.

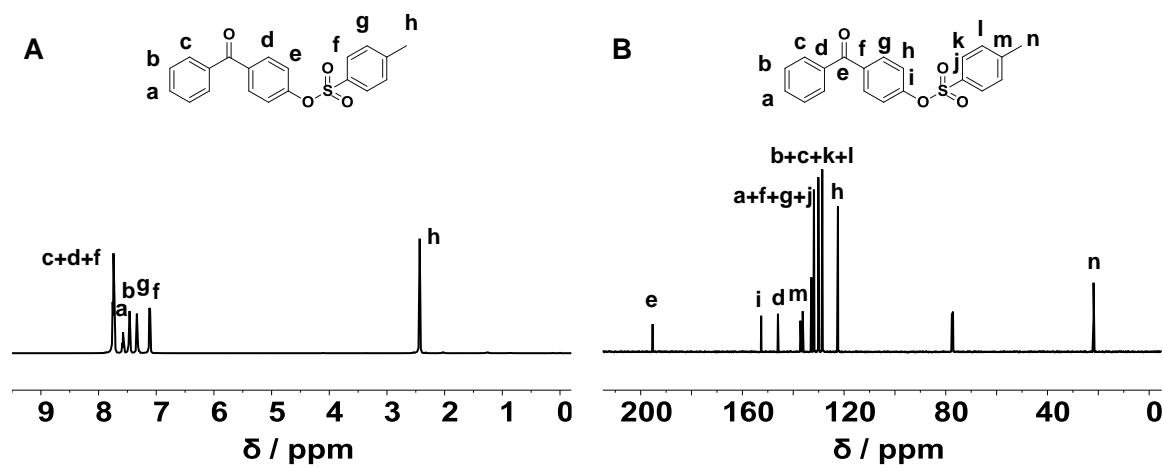


Figure S11. Structural characterization of 4-toluenesulfonylbenzophenone: ^1H NMR spectrum (A) and ^{13}C NMR spectrum (B), related to **Figure 4**.

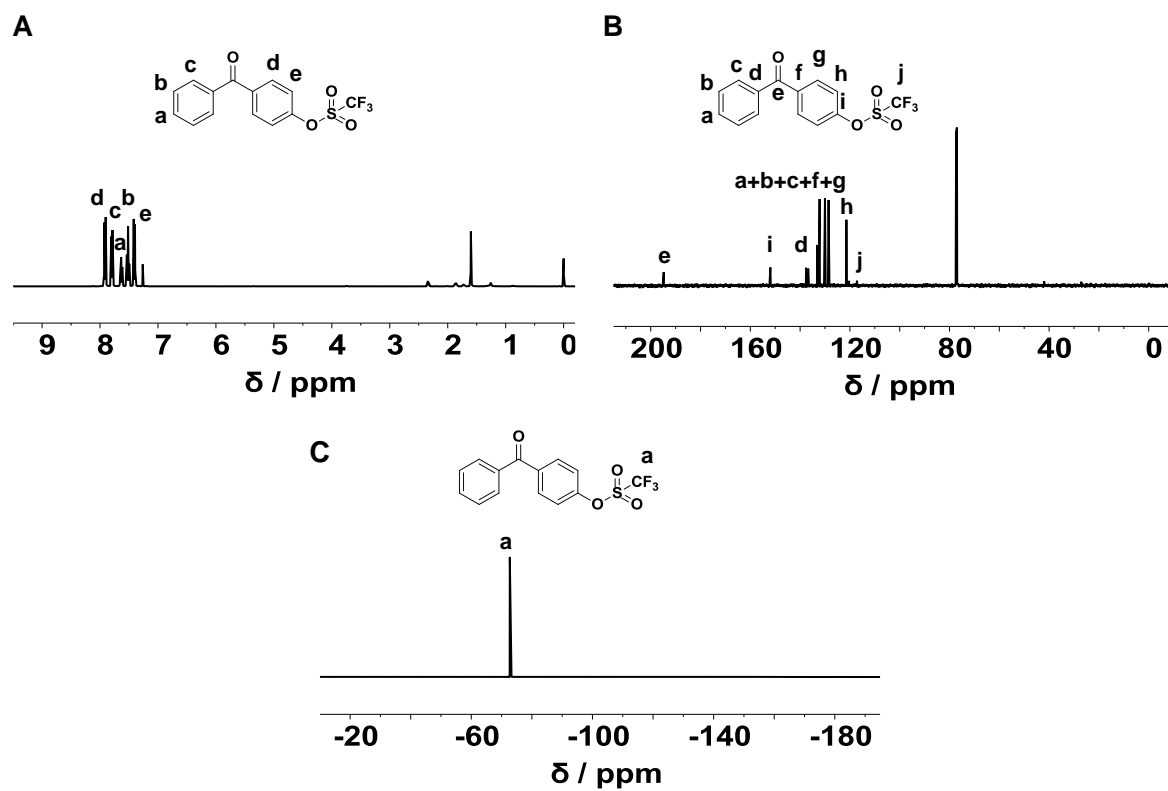


Figure S12. Structural characterization of 4-(trifluoromethylsulfonyl)benzophenone: ^1H NMR spectrum (A), ^{13}C NMR spectrum (B) and ^{19}F NMR spectrum (C), related to **Figure 4**.

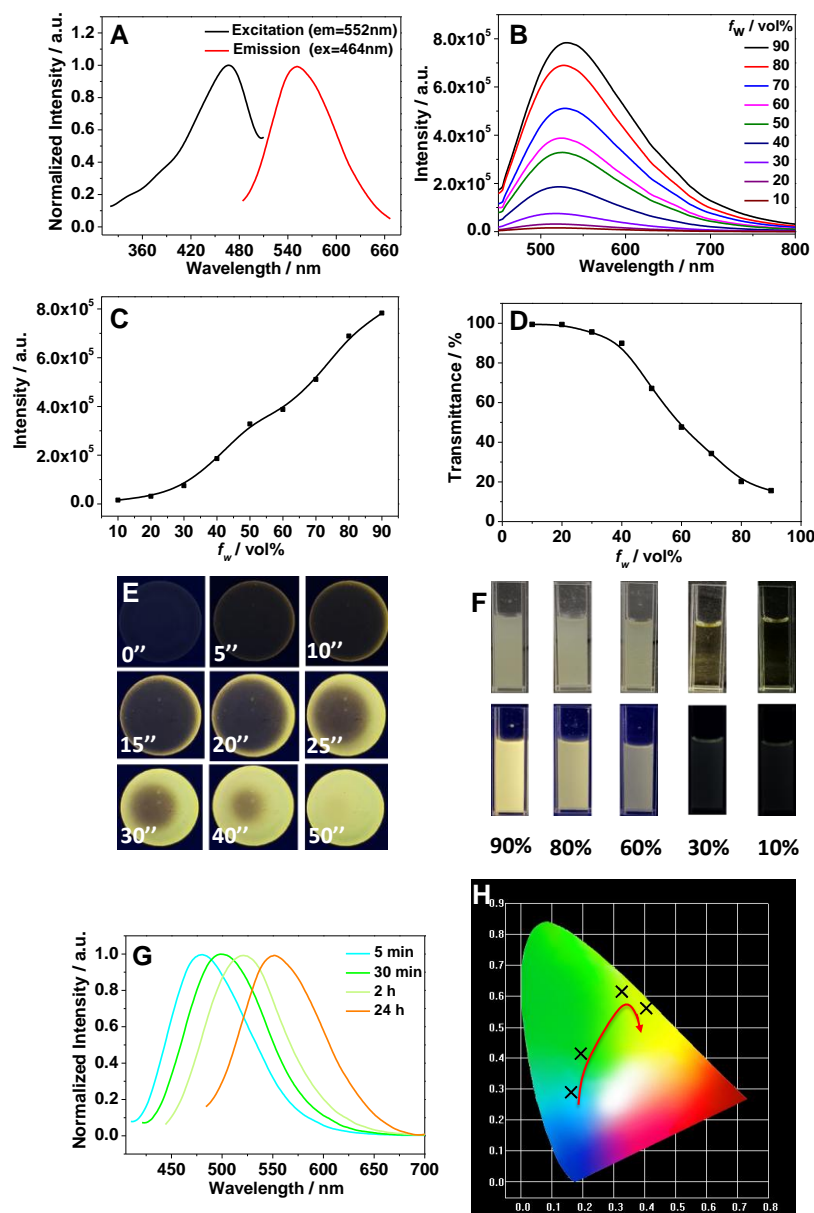


Figure S13. Fluorescence properties of PTPMs. Excitation and emission spectra of CF₃-PTPM in the solid state (A). Emission spectra of CF₃-PTPM (0.1 mg/mL) in water/THF mixtures with different water volume fractions (f_w , vol %) (excited at 425 nm) (B). Plots of emission intensities of CF₃-PTPM (0.1 mg/mL) in water/THF mixtures with different water volume fractions (f_w , vol %) (excited at 425 nm) (C). Transmittance of CF₃-PTPM (0.1 mg/mL) in water/THF mixtures with different water volume fractions (f_w , vol %) at 650 nm wavelength (D). Digital photos of one drop of CF₃-PTPM solution (10 mg/mL in THF) on thin-layer chromatography at different times (time unit is second) of evaporation (under UV irradiation at 365 nm) (E). Digital photos of CF₃-PTPM (0.1 mg/mL) in water/THF mixtures with different water volume fractions (f_w , vol %) (under sunlight and UV irradiation at 365 nm) (F). Emission spectra of CF₃-PTPM obtained at different polymerization times (G). CIE coordinates of CF₃-PTPM obtained at different polymerization times (H), related to **Figure 4**.

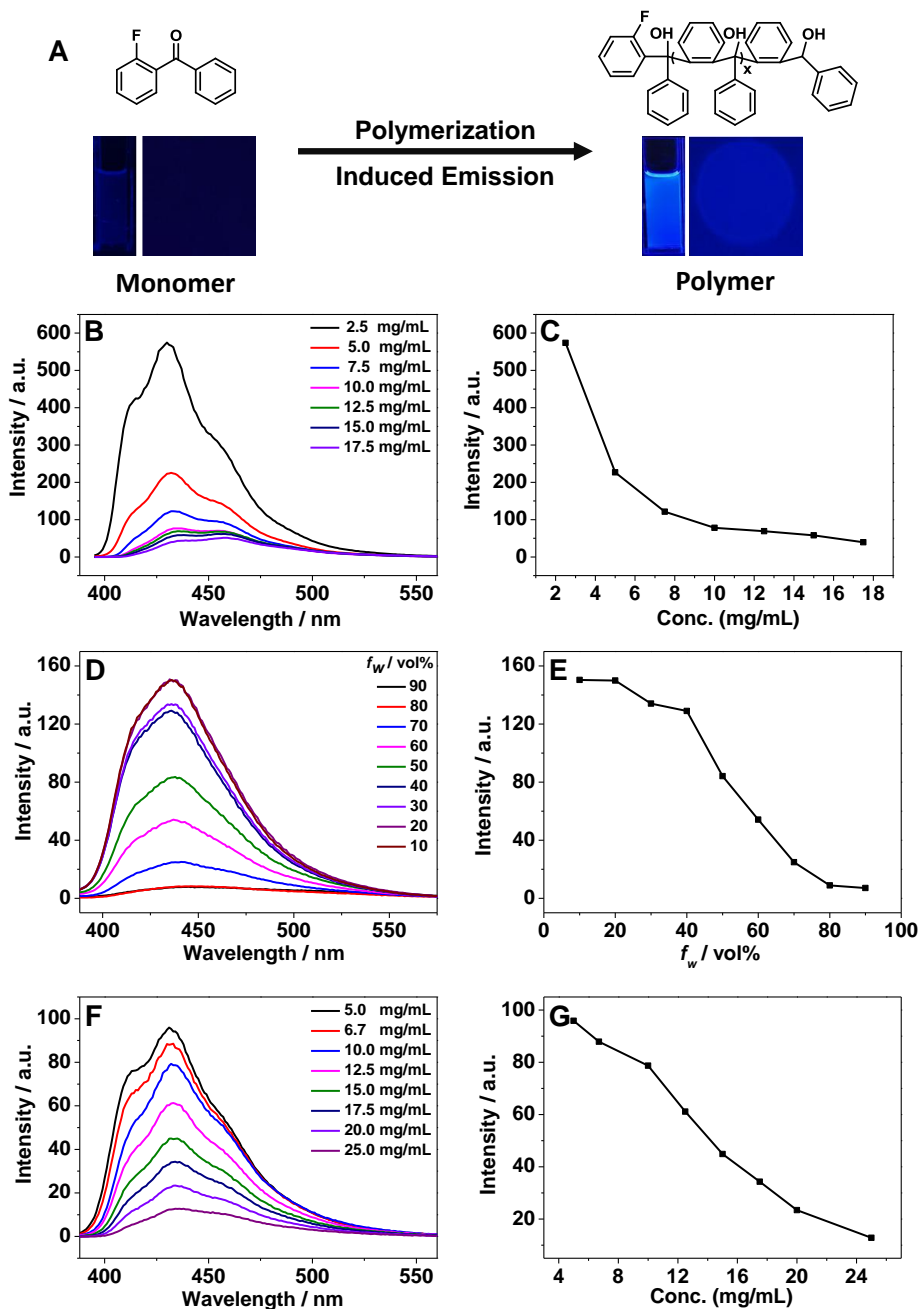


Figure S14. Photophysical properties of 2-fluoro-PTPM solution in THF. Chemical structure and emission digital photos (under irradiation with UV lamp at 365 nm) of polymerization process of 2-fluorobenzophenone (A), emission spectra at different concentration (excited at 375 nm) (B) and plots of fluorescent intensity (C) of polymers at a polymerization time of 12 h, emission spectra of 2-fluoro-PTPM (0.1 mg/mL) in water/THF mixtures with different water volume fractions (f_w , vol%) (D) and plots of fluorescent intensities (E) of polymers at a polymerization time of 24 h, emission spectra at different concentration (excited at 375 nm) (F) and plots of fluorescent intensity (G) of polymers at a polymerization time of 24 h, related to **Figure 4**.

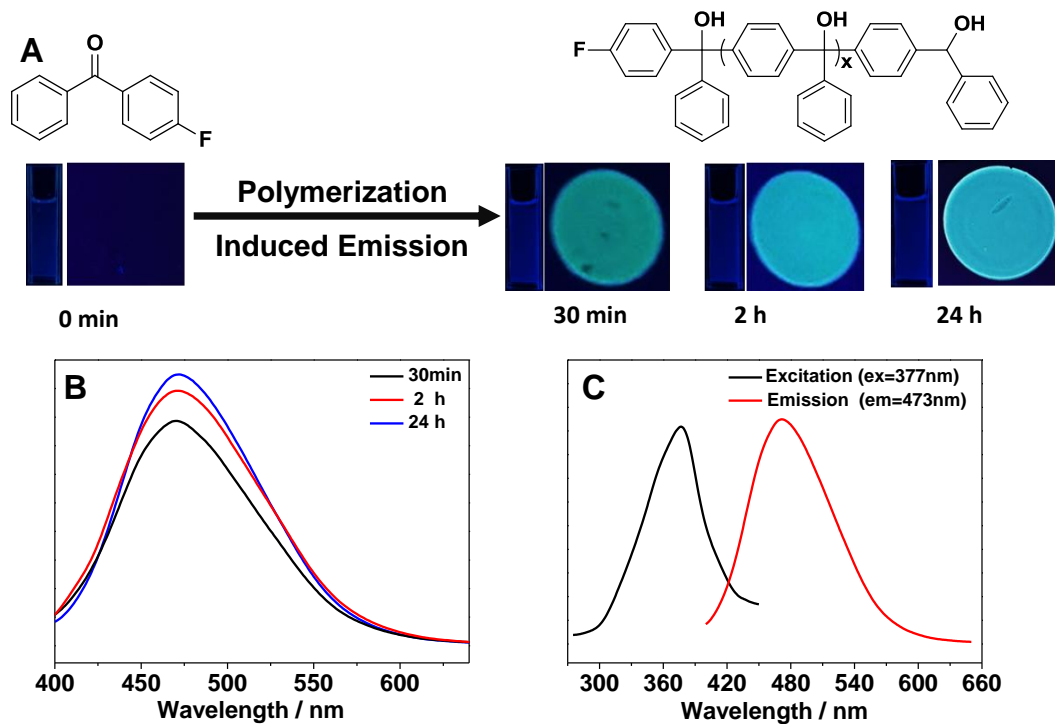


Figure S15. Polymerization-induced emission property of fluoro-PTPM. Emission digital photos (under irradiation with UV lamp at 365 nm) of polymerization process of 4-fluorobenzophenone at different polymerization times (A), emission spectra of fluoro-PTPM obtained at different polymerization times and digital photos (under UV irradiation at 365 nm) (B), excitation and emission spectra in the solid state (C), related to **Figure 4**.

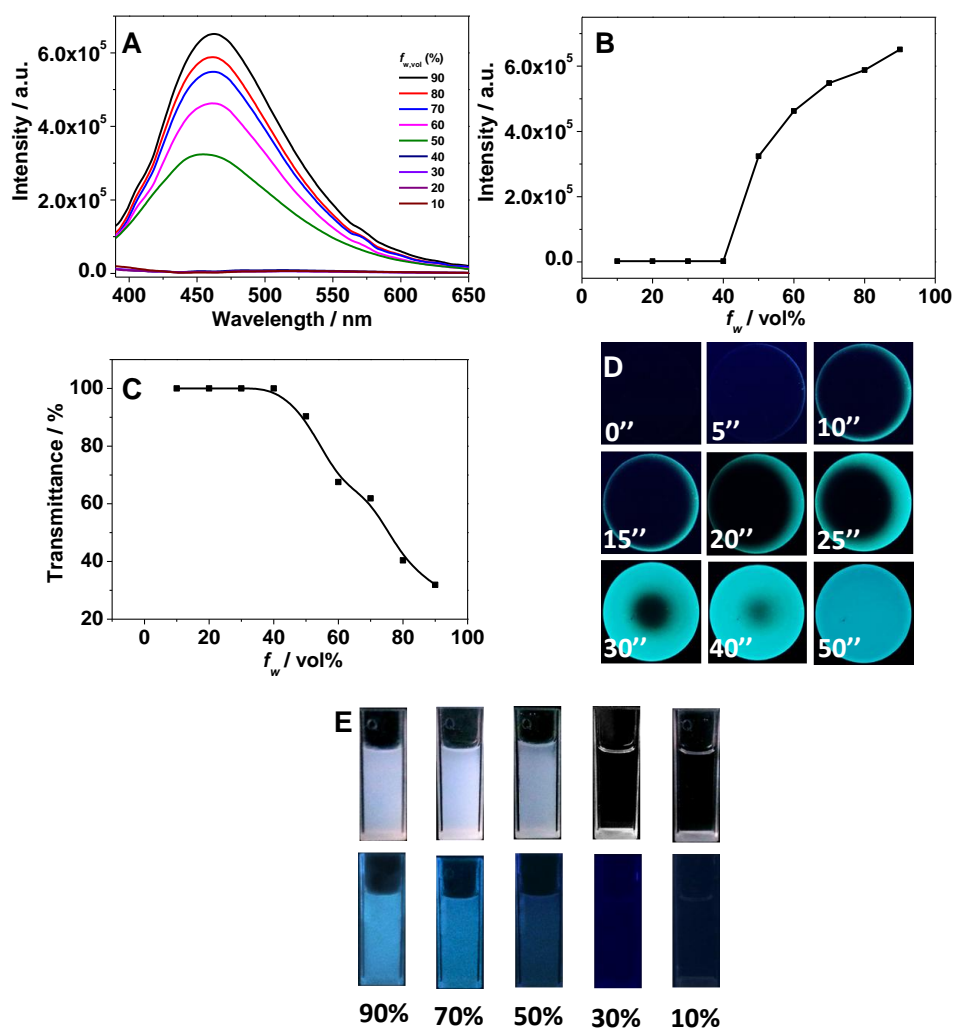


Figure S16. Aggregation-induced emission property of fluoro-PTPM. Emission spectra of fluoro-PTPM (0.1 mg/mL) in water/THF mixtures with different water volume fractions (f_w , vol %) (excited at 440 nm) (A), plots of emission intensities of fluoro-PTPM (0.1 mg/mL) in water/THF mixtures with different water volume fractions (f_w , vol %) (excited at 440 nm) (B), transmittance of fluoro-PTPM (0.1 mg/mL) in water/THF mixtures with different water volume fractions (f_w , vol %) at 650 nm wavelength (C), digital photos of one drop of fluoro-PTPM solution (10 mg/mL in THF) on thin-layer chromatography at different times (time unit is second) of evaporation (under UV irradiation at 365 nm) (D), digital photos of fluoro-PTPM (0.1 mg/mL) in water/THF mixtures with different water volume fractions (f_w , vol %) (under sunlight and UV irradiation at 365 nm) (F), related to **Figure 4**.

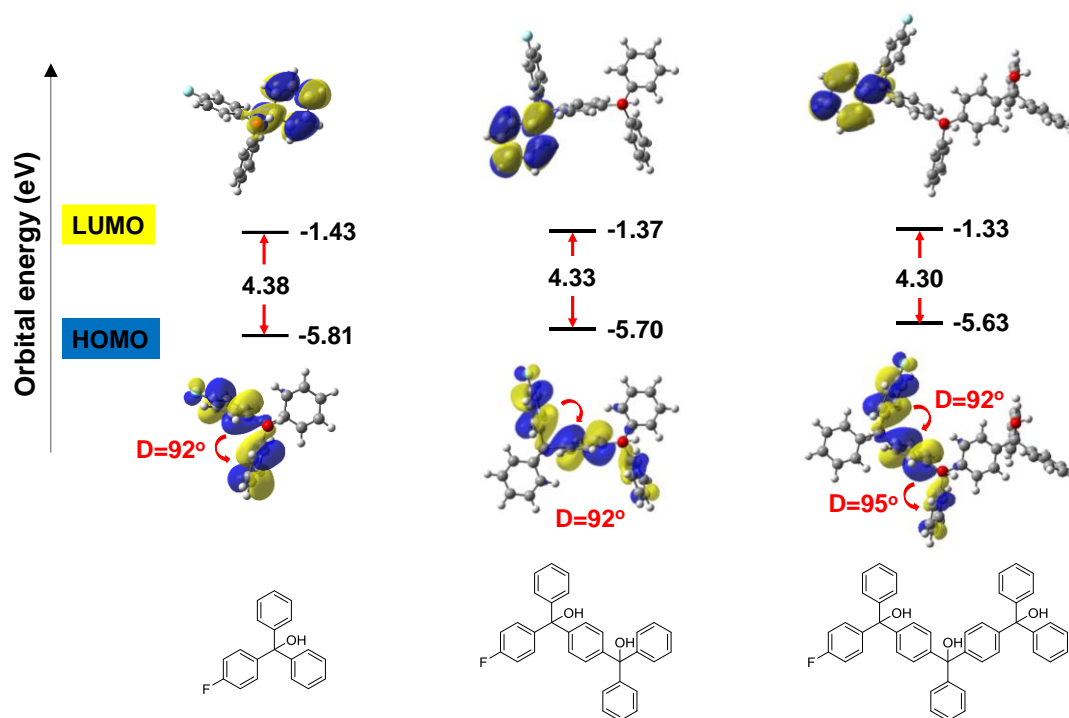


Figure S17. Electron cloud distributions and energy levels (eV) of fluoro-TPM, fluoro-TPM dimer and fluoro-TPM trimer in the excited state calculated by TD-DFT B3LYP/6-311G*, Gaussian 09 program. D: dihedral angle, related to **Figure 4**.

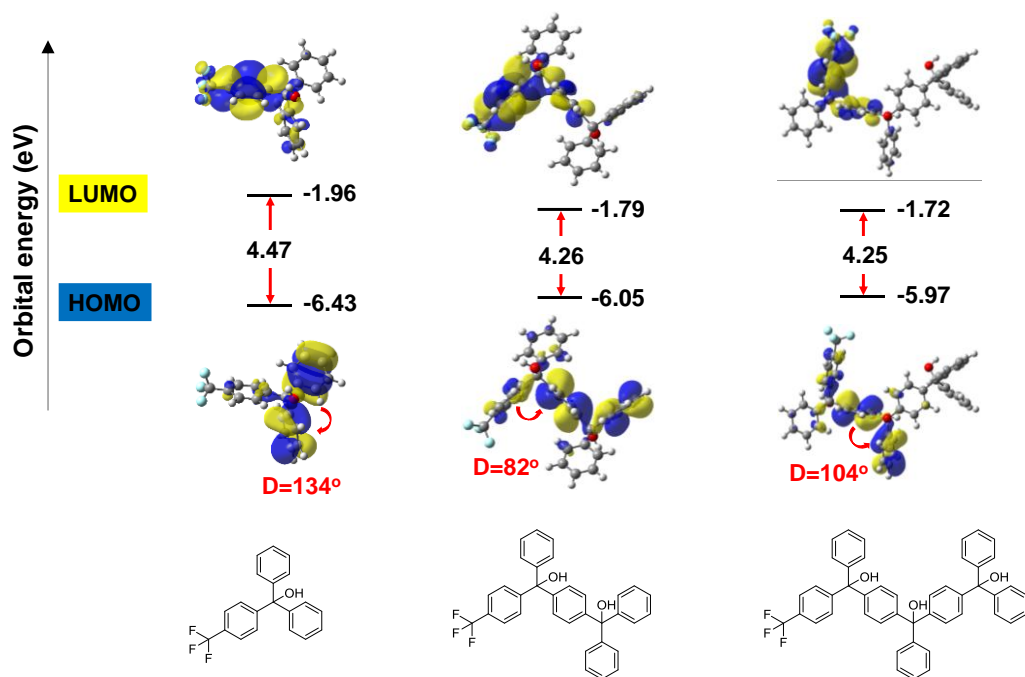


Figure S18. Electron cloud distributions and energy levels (eV) of trifluoromethyl-TPM, trifluoromethyl-TPM dimer and trifluoromethyl-TPM trimer in the excited state calculated by TD-DFT B3LYP/6-311G*, Gaussian 09 program. D: dihedral angle, related to **Figure 4**.

NMR Spectra

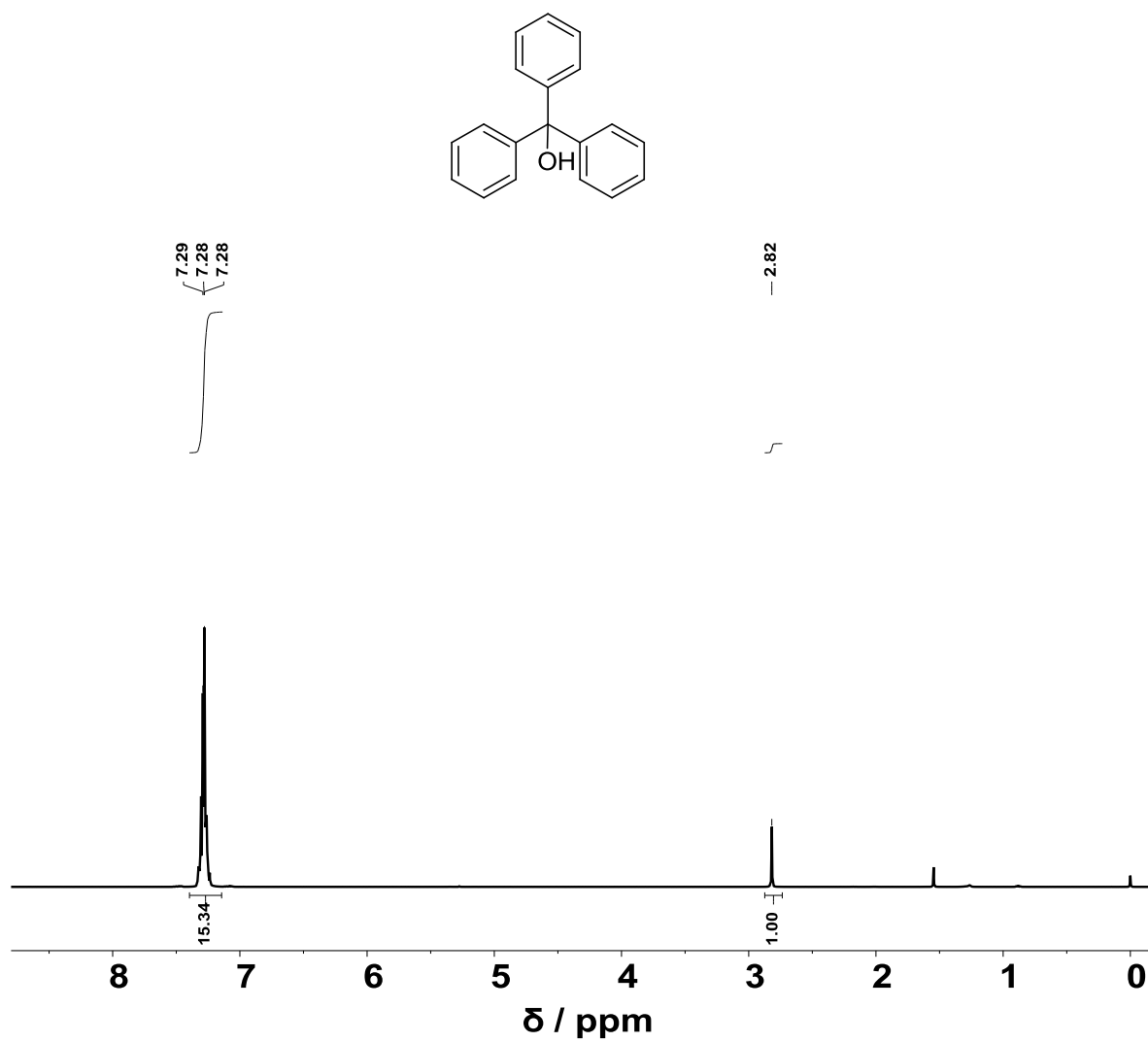


Figure S19. ¹H NMR spectrum of compound TPM, related to Figure 1.

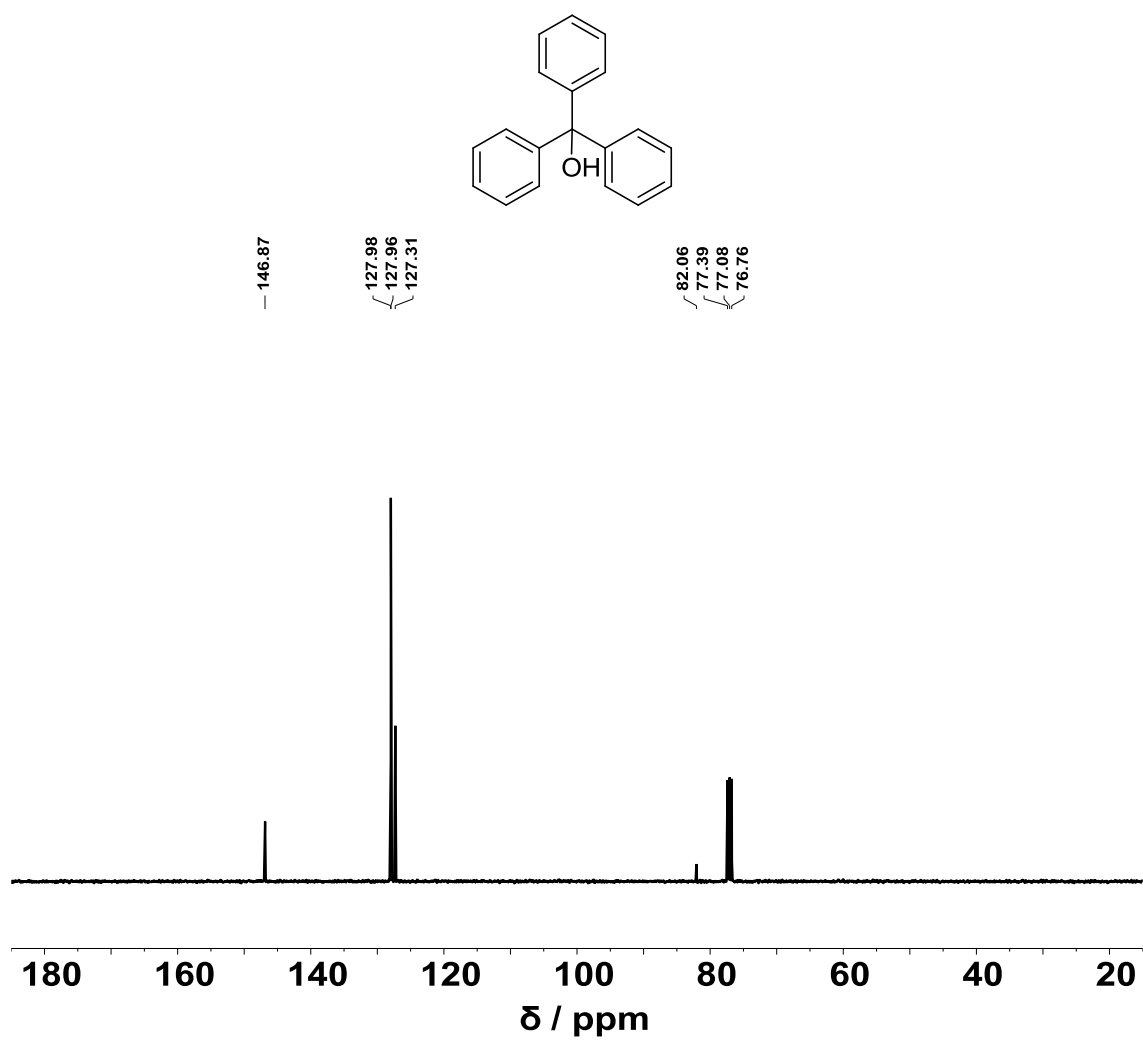


Figure S20. ¹³C NMR spectrum of compound TPM, related to Figure 1.

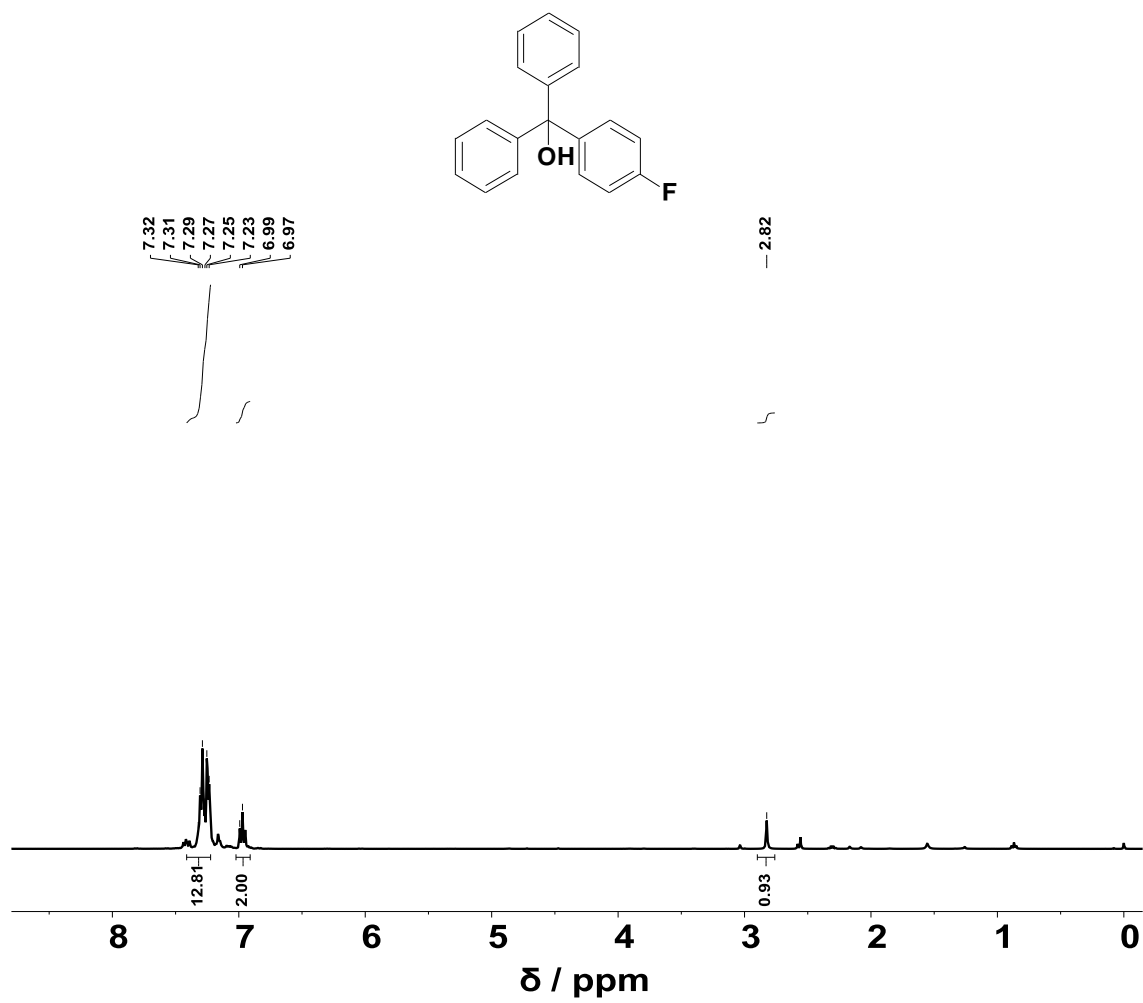


Figure S21. ¹H NMR spectrum of compound **F-TPM**, related to **Figure 1**.

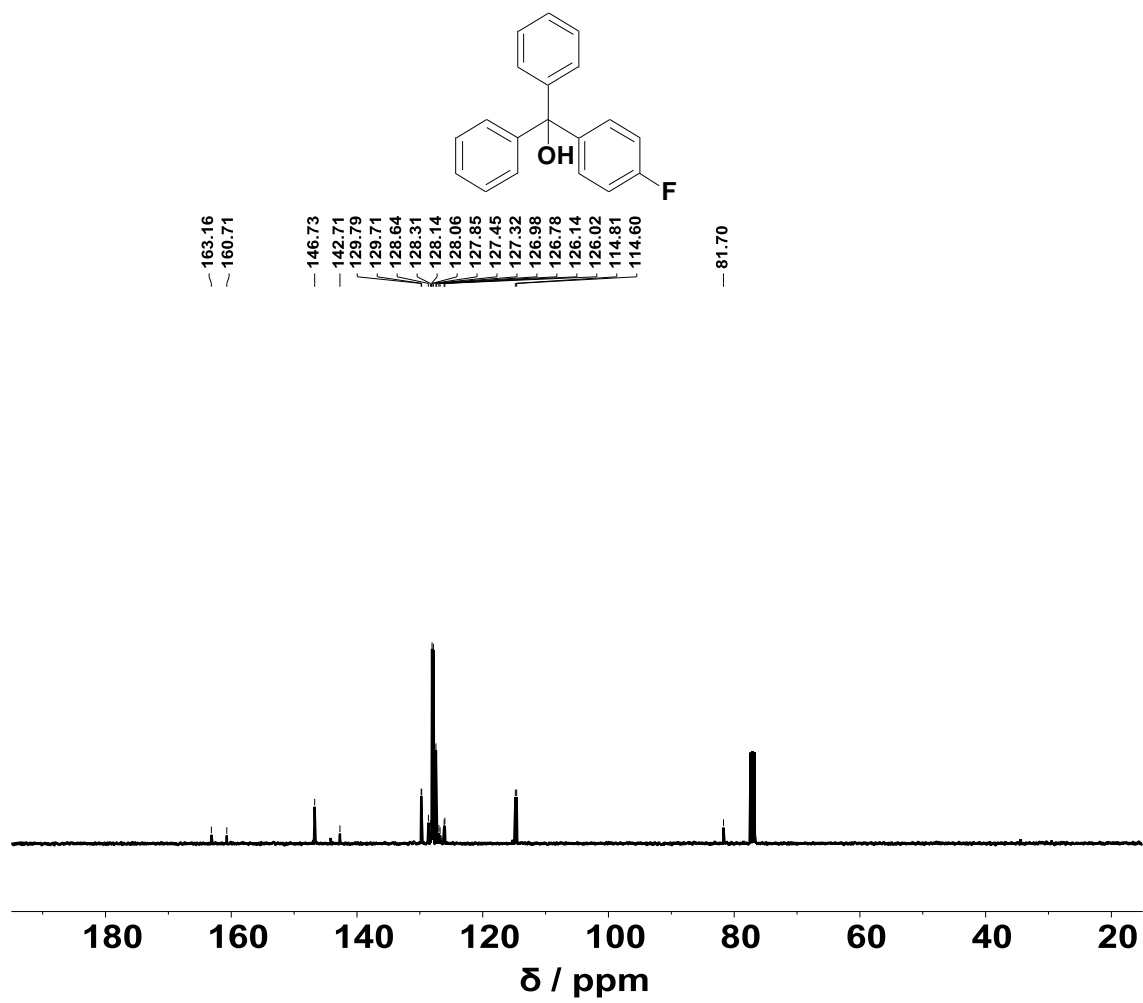


Figure S22. ¹³C NMR spectrum of compound F-TPM, related to Figure 1.

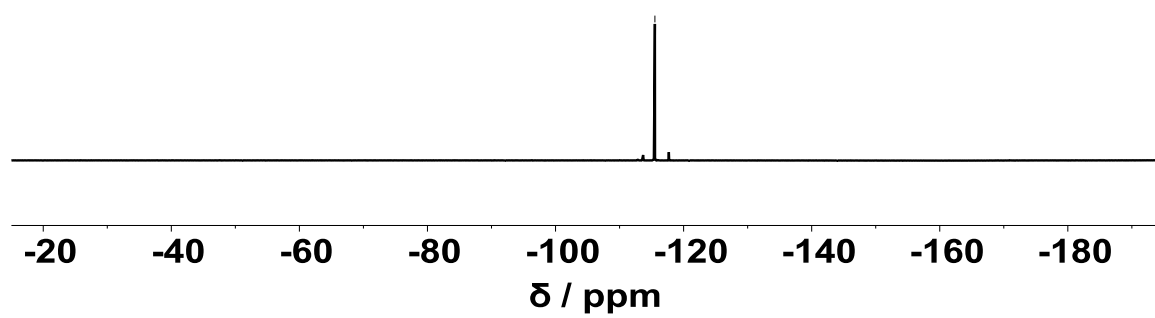
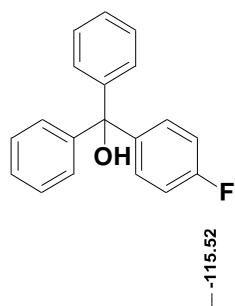


Figure S23. ^{19}F NMR spectrum of compound **F-TPM**, related to **Figure 1**.

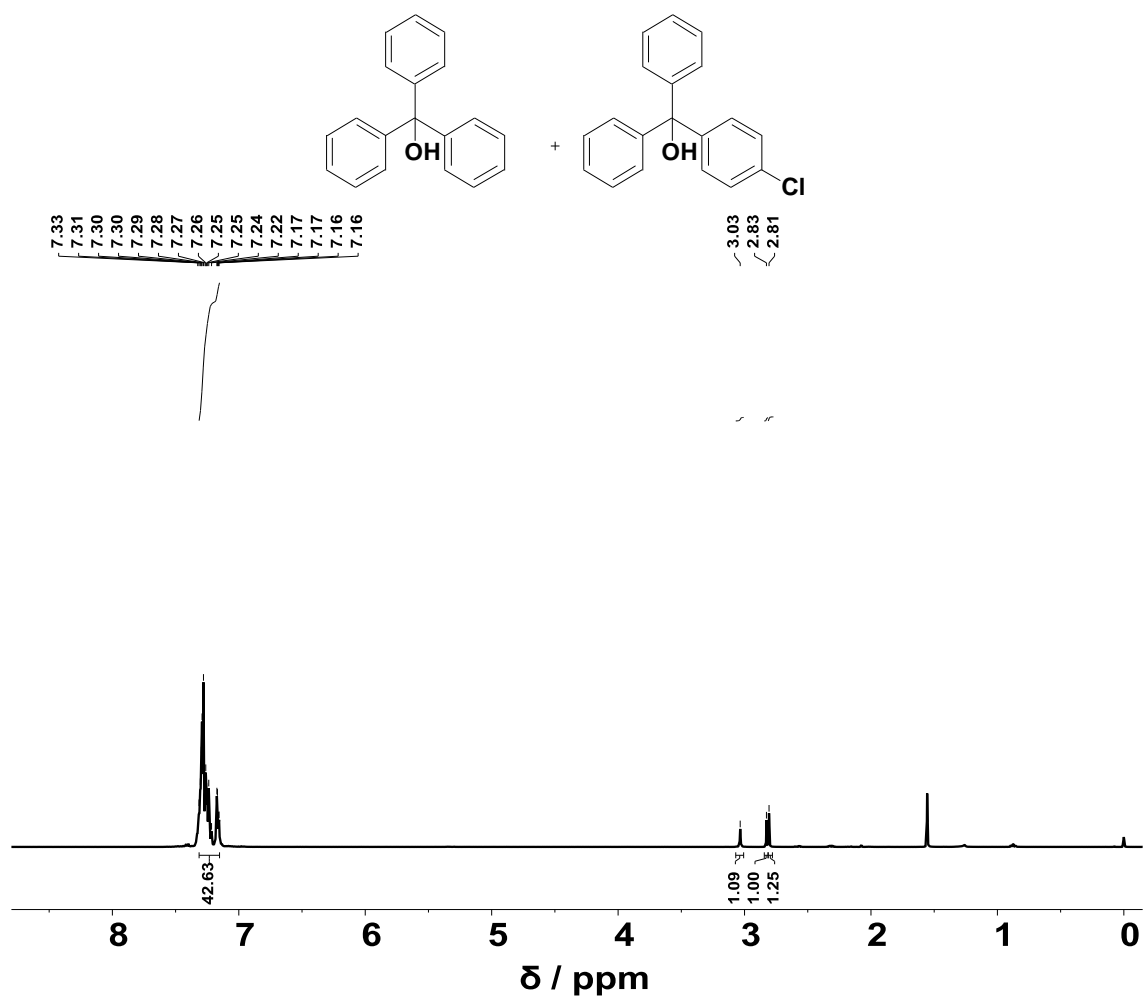


Figure S24. ¹H NMR spectrum of compound TPM and Cl-TPM, related to **Figure 1**.

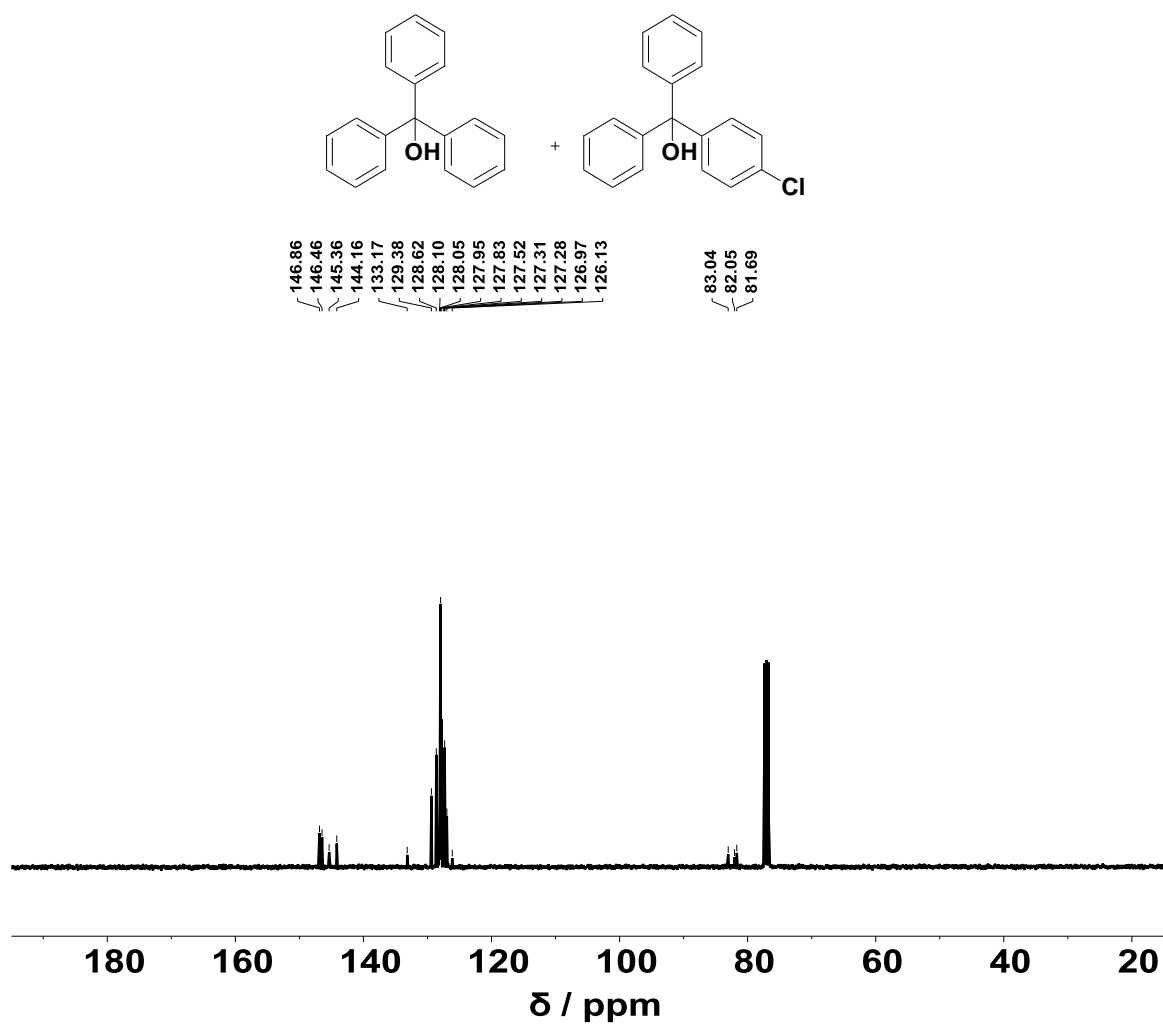


Figure S25. ^{13}C NMR spectrum of compound TPM and Cl-TPM, related to Figure 1.

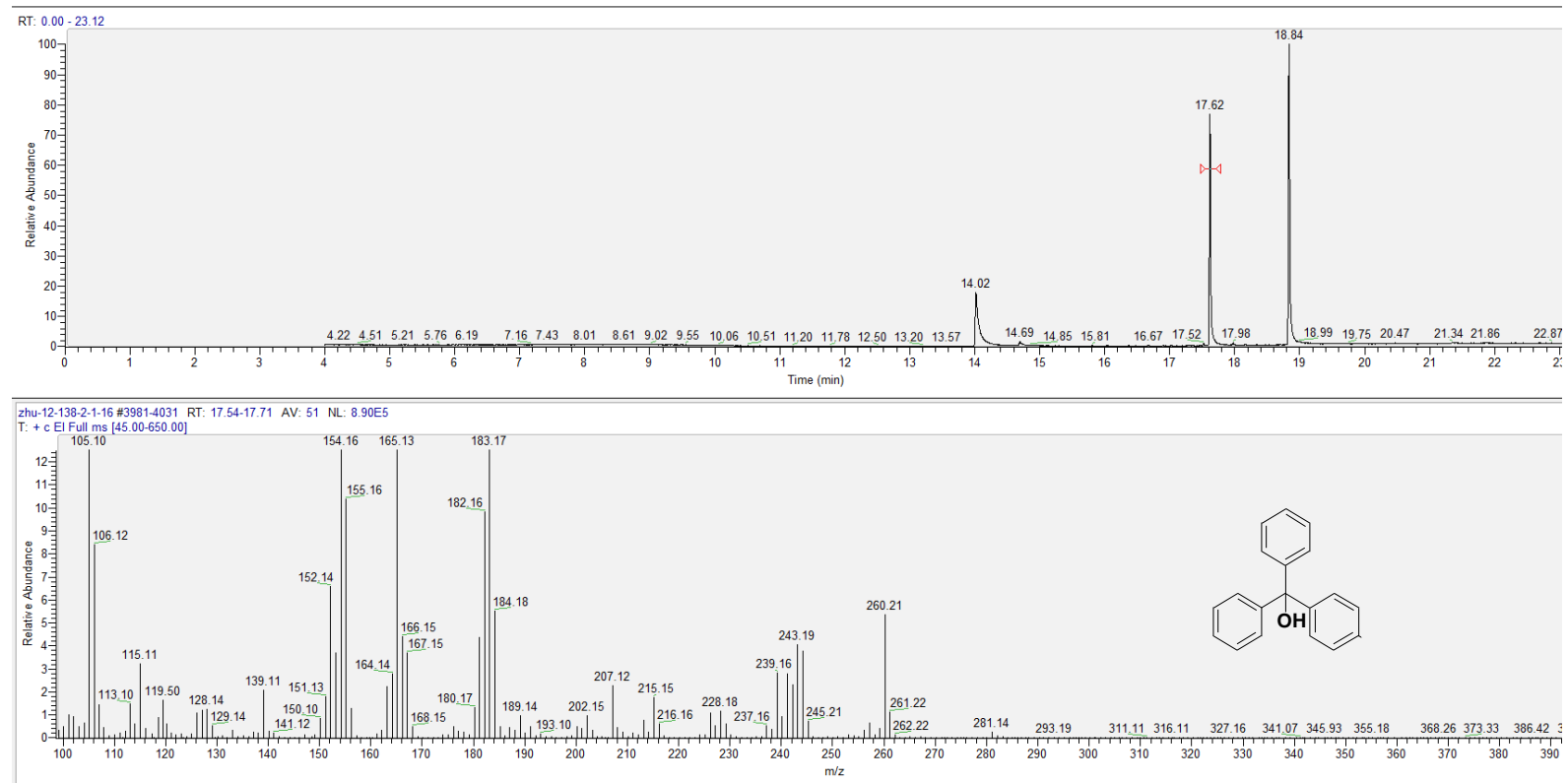


Figure S26. GC-MS characterization of compound **TPM**, related to **Figure 1**.

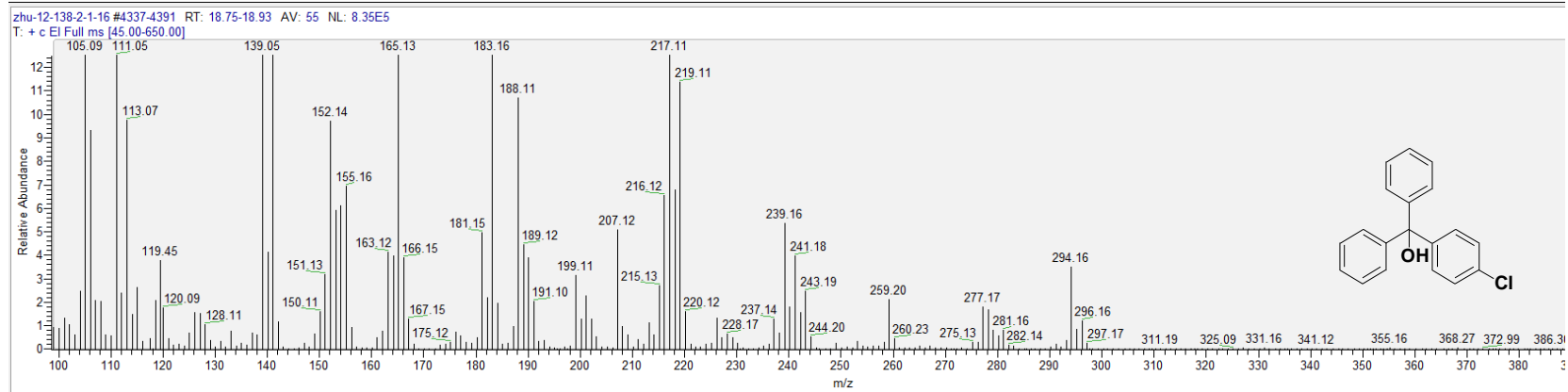
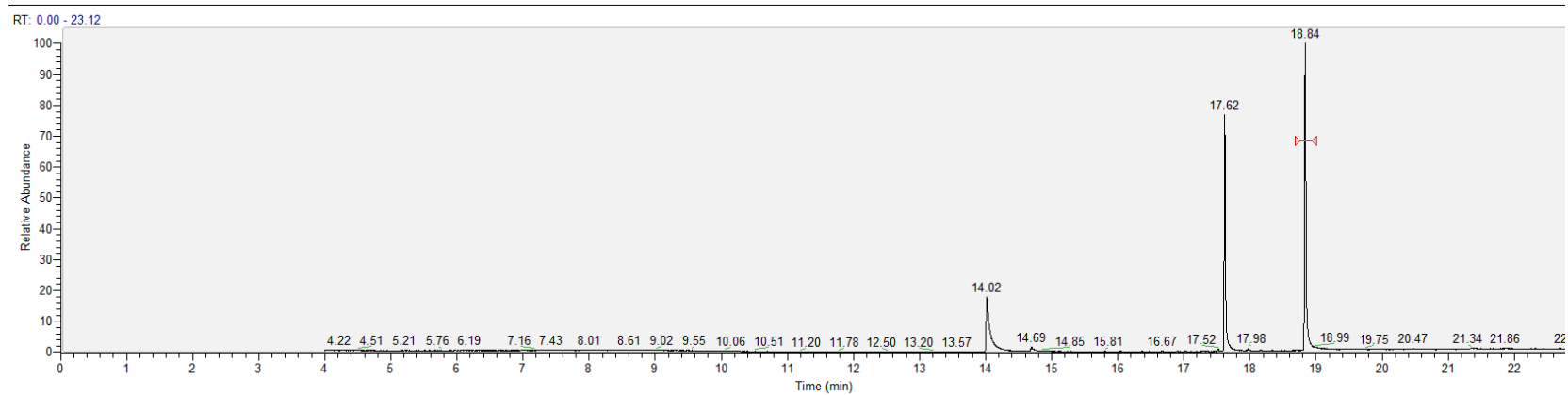


Figure S27. GC-MS characterization of compound **Cl-TPM**, related to **Figure 1**.

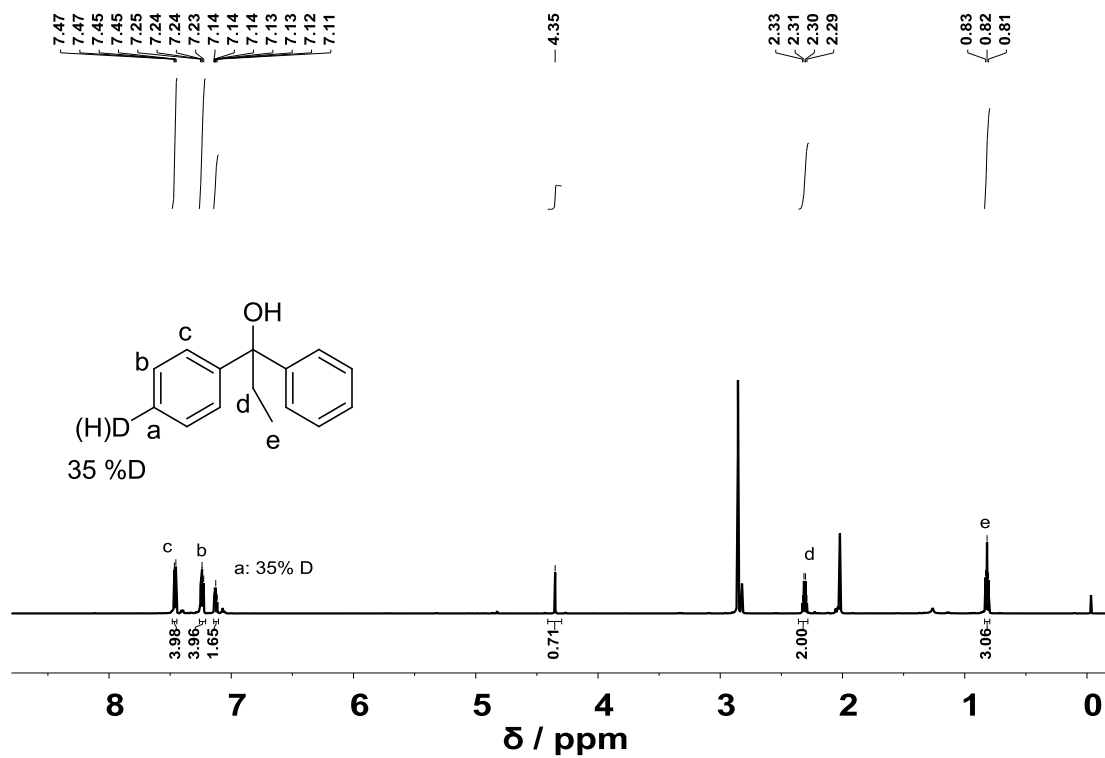


Figure S28. ^1H NMR spectrum of *para*-deuterated diphenylethylmethanol, related to Figure 3.

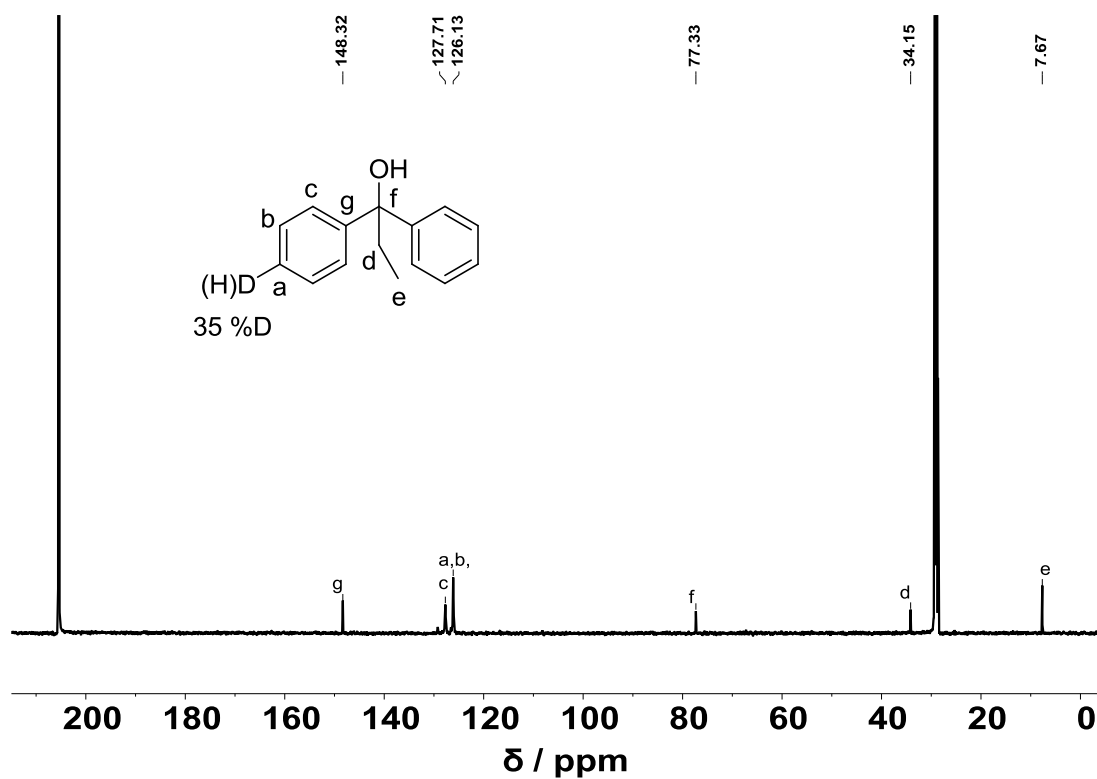


Figure S29. ^{13}C NMR spectrum of *para*-deuterated diphenylethylmethanol, related to Figure 3.

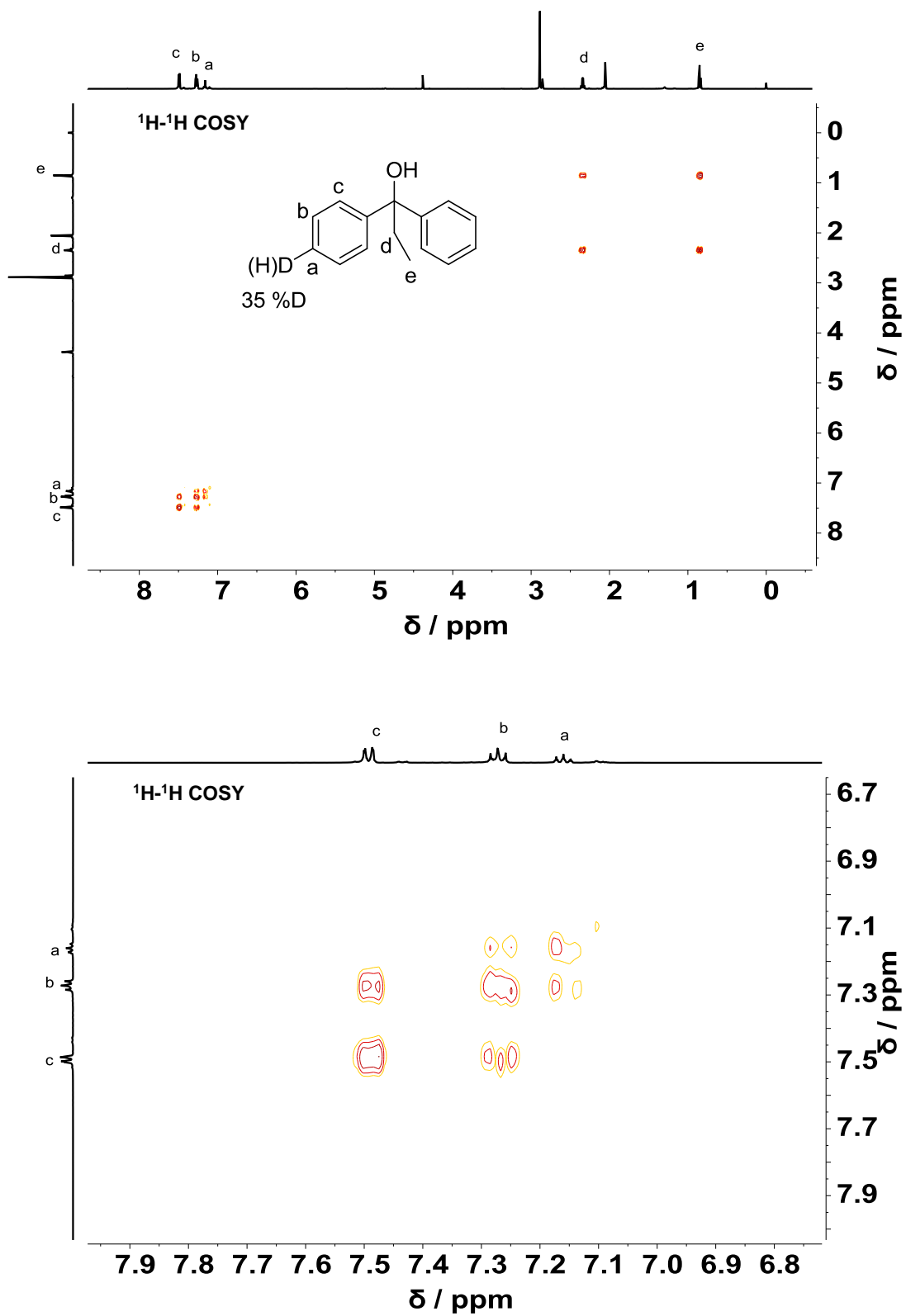


Figure S30. ^1H - ^1H COSY NMR spectra of para-deuterated diphenylethylmethanol, related to Figure 3.

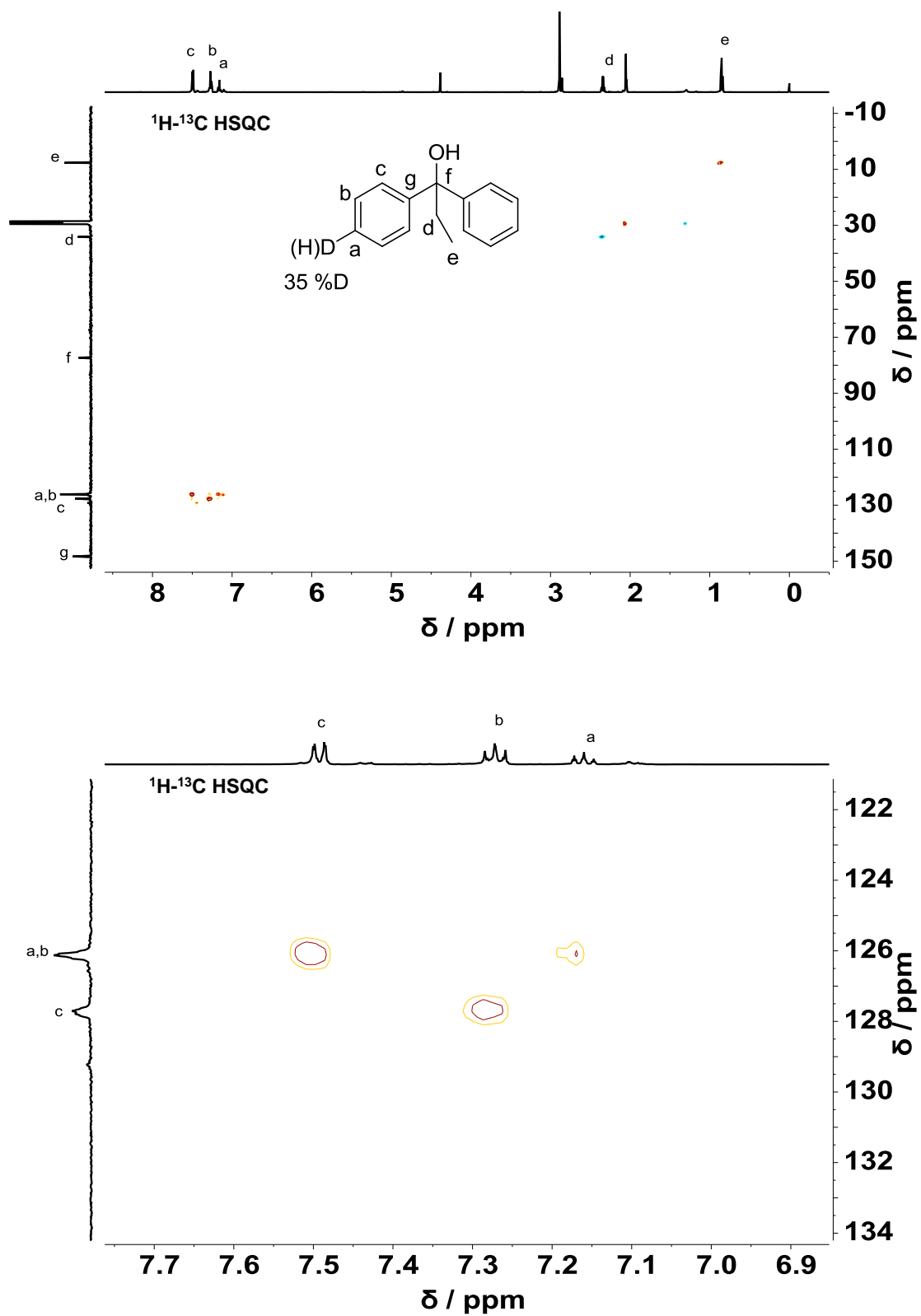


Figure S31. ^1H - ^{13}C HSQC NMR spectra of para-deuterated diphenylethylmethanol, related to **Figure**

3.

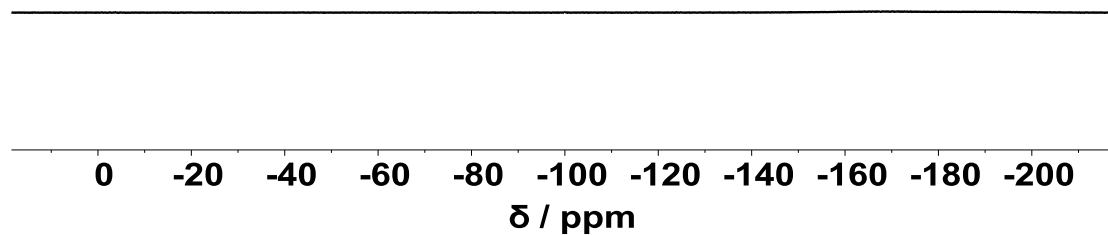
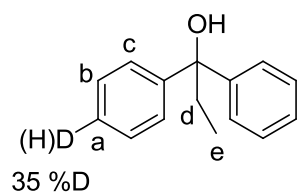
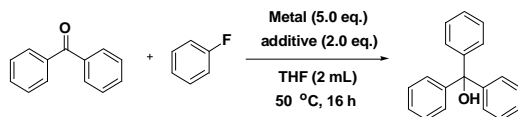


Figure S32. ^{19}F NMR spectrum of para-deuterated diphenylethylmethanol, related to **Figure 3**.

Supplemental Tables

Table S1. The influence of catalysts, additives and solvents on Mg-mediated C-F activation, related to **Figure 1**.



Entry	Metal	Additive (X eq.)	Solvent(2 mL)	Yield /% ^[a]
1	Mg	LiCl (2.0 eq.)	THF	15
2	In	LiCl (2.0 eq.)	THF	Trace
3	Zn	LiCl (2.0 eq.)	THF	Trace
4	Mn	LiCl (2.0 eq.)	THF	Trace
5	--	LiCl (2.0 eq.)	THF	Trace
6	Mg	LiCl (2.0 eq.)	Toluene	Trace
7	Mg	LiCl (2.0 eq.)	Dioxane	Trace
8	Mg	LiCl (2.0 eq.)	DME	Trace
9	Mg	LiCl (2.0 eq.)	CH ₃ CN	Trace
10	Mg	LiCl (2.0 eq.)	Ether	Trace
11	Mg	LiCl (2.0 eq.)	Tert-Butyl methyl ether (MTBE)	Trace
12	Mg	LiCl (2.0 eq.)	Isopropyl ether	Trace
13	Mg	BrCH ₂ CH ₂ Br (0.2 eq.)	THF	25
14	Mg	BrCH ₂ CH ₂ Br (2.0 eq.)	THF	6
15	Mg	NaI (2.0 eq.)	THF	Trace
16	Mg	LiI (2.0 eq.)	THF	Trace
17	Mg	InCl ₃ (2.0 eq.)	THF	Trace
18	Mg	NaCl (2.0 eq.)	THF	Trace
19	Mg	SnCl ₂ · 2H ₂ O (2.0 eq.)	THF	Trace
20	Mg	LiClO ₄ (2.0 eq.)	THF	Trace
21	Mg	AlCl ₃ (2.0 eq.)	THF	Trace
22	Mg	ZnCl ₂ (2.0 eq.)	THF	Trace
23	Mg	FeCl ₃ (2.0 eq.)	THF	Trace
24	Mg	TiCl ₄ (2.0 eq.)	THF	Trace
25	Mg	RhCl ₃ (2.0 eq.)	THF	Trace
26	Mg	HgCl ₂ (2.0 eq.)	THF	Trace
27	Mg	PbCl ₂ (2.0 eq.)	THF	Trace
28	Mg	NiCl ₂ (2.0 eq.)	THF	Trace
29	Mg	CuI (2.0 eq.)	THF	Trace
30	Mg	CeCl ₃ (2.0 eq.)	THF	Trace
31	Mg	TiCl ₄ (2.0 eq.)	THF	Trace
32	Mg	KI (2.0 eq.)	THF	Trace
33	Mg	KBr (2.0 eq.)	THF	Trace
34	Mg	LiCl (0.2 eq.)	THF	Trace

[a] isolated yield.

Table S2. Reactivity of fluorobenzene with different substrates in the Barbier reaction (A) and the Grignard reaction (B), related to **Figure 1**.

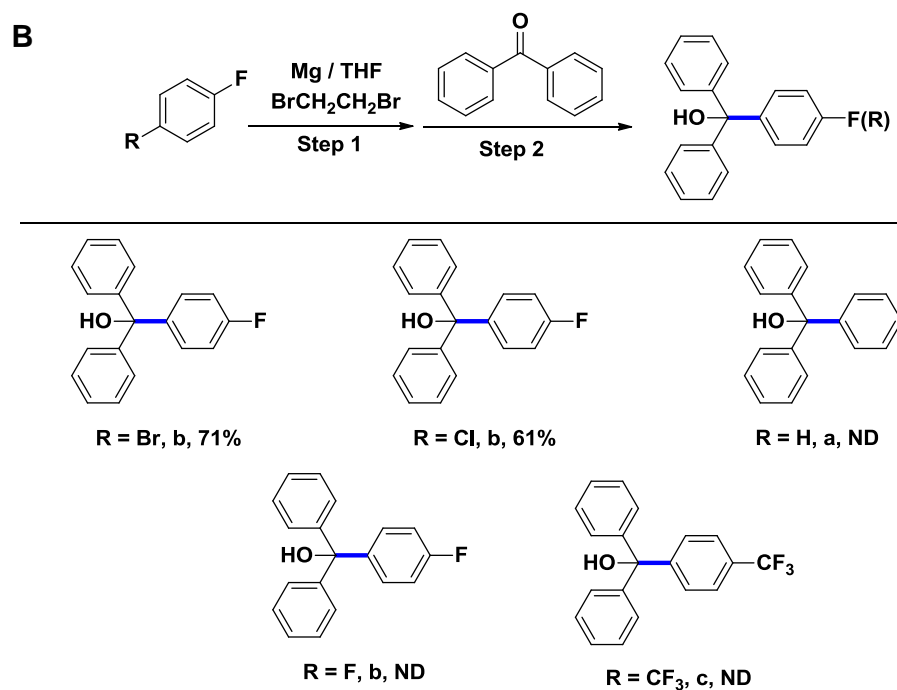
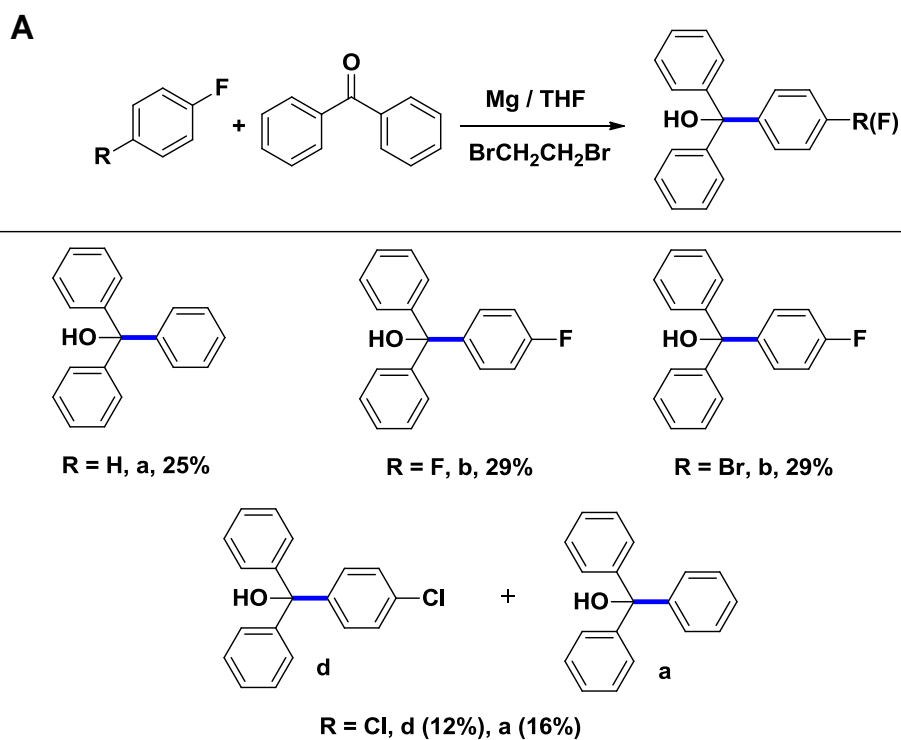


Table S3. Reactivity of C-F, C-Cl and C-Br in Barbier reaction and Grignard reaction, related to **Figure 1.**

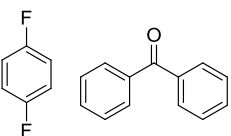
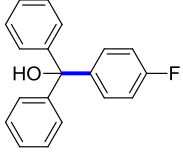
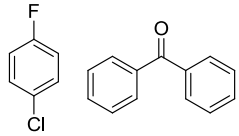
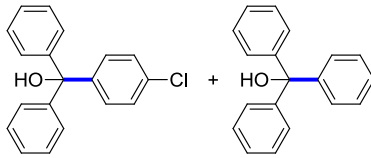
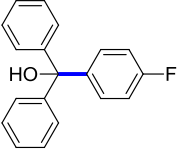
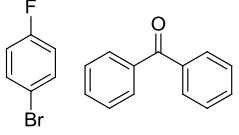
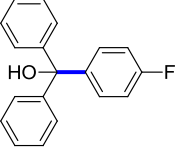
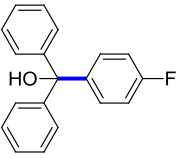
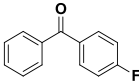
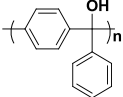
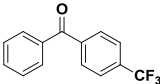
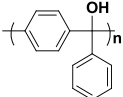
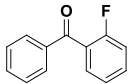
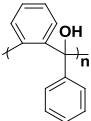
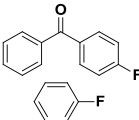
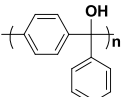
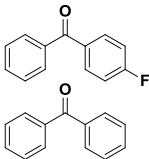
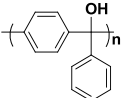
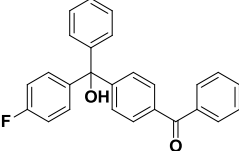
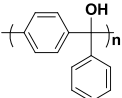
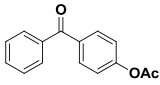
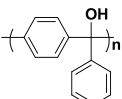
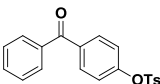
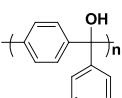
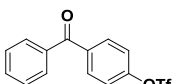
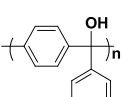
Entry	Reactant	Reaction Type	Product and Yield
1		Barbier reaction	 29%
		Grignard reaction	—
2		Barbier reaction	 12% 16%
		Grignard reaction	 61%
3		Barbier reaction	 29%
		Grignard reaction	 71%

Table S4. Monomer structures and results of polymers synthesized via self-condensing ketyl polymerization, related to **Figure 4**.

Entry	Monomer	Polymer	Conversion(%) ^[a]	Yield(%)	M_n ^[b]	\bar{D}	PIE ^[c]
1			89.9	70.0	3400	1.40	AIE
2			92.5	71.4	4900	1.38	AIE
3			86.2	62.5	3800	1.25	ACQ
4			88.5	68.8	3300	1.38	AIE
5			N/A	N/A	N/A	N/A	N/A
6			N/A	N/A	N/A	N/A	N/A
7			N/A	N/A	N/A	N/A	N/A
8			N/A	N/A	N/A	N/A	N/A
9			N/A	N/A	N/A	N/A	N/A

[a] calculated from ¹H NMR spectroscopy by comparing the integral ratio between terminal group and polymer;

[b] measured by GPC;

[c] polymerization-induced emission.

Transparent Methods

Materials

All chemicals and reagents were purchased from commercial suppliers and used without further purification. THF was distilled from Na/benzophenone prior to use.

Characterization methods

Nuclear magnetic resonance (NMR) spectroscopy. The NMR spectroscopy was performed on Bruker Ascend TM 400 or ECZ600S spectrometer, which CDCl_3 was used as solvent and tetramethylsilane as an internal standard. Respectively, ^1H NMR measured at concentration of 10-20 mg/mL, ^{13}C NMR at concentration of 60-80 mg/mL and ^{19}F NMR at concentration of 40-60 mg/mL.

Gel permeation chromatography (GPC). GPC curves of F-PTPMs were performed on a Viscotek TDA 302 triple detector array equipped with one TSK-Gel GMHHR-N column, which aimed at determined the molecular weight and molecular weight distribution. In detail, THF was used as eluent at a flow rate of 1.0 mL/min and carried out at 30 °C. Monodispersed polystyrene standards were used in the calibration of molecular weight and molecular weight distribution.

Fourier transform infrared (FT-IR) spectroscopy. FT-IR spectra were performed on a TENSOR II FT-IR Spectrometre (Bruker, Germany). The spectra were collected at room temperature and recorded from an accumulation of 16 scans in the range of 4000-400 cm^{-1} . The OPUS v7.5 software auto-corrected the spectral base line and calculated the second derivative spectra.

Differential scanning calorimeter (DSC) curve. Thermal characterization was performed on a DSC214 polyma (NETZSCH, Germany). The test atmosphere and purge gas were high pure N_2 , and the flow rate of N_2 was 60 mL/min. An empty Al crucible was used as the reference. The temperature range of test was 25-200°C with a heating rate of 10 K/min, and the cooling rate was 10 K/min. After removing the thermal history of the material by raise and cool down twice, the thermodynamic curves were measured.

MALDI-TOF mass spectrometry. Mass spectrum was recorded on a Microflex MALDI-TOF mass spectrometer (Bruker Daltonics) in the positive-ion mode.

High-resolution mass spectrometry. HRMS data were recorded on Waters Micromass GCT Premier.

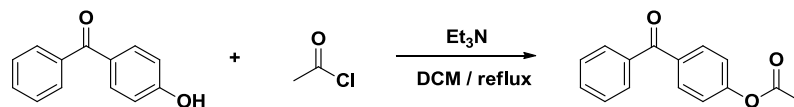
UV-vis absorption. Sample transmittance recorded on a Shimadzu UV-2450 UV-Vis spectrophotometer at room temperature in THF/Water mixtures with different water fractions (f_w , vol%).

Photophysical properties. The measurement of the polymers in solvent/nonsolvent mixtures were tested. In this study, THF was selected as good solvent for polymers and water as aggregation-inducing nonsolvent. The fluorescence spectra of polymers in THF/Water mixtures with different water content were recorded respectively on an Edinburgh Instruments FLS5 fluorescence spectrofluorometer and Shimadzu Instruments RF-5301PC fluorescence spectrophotometer.

Theoretical calculation. The hybrid density functional theory B3LYP with Grimme's dispersion correction (DFT-D3) was employed for all geometrical optimizations, thermal energy calculations and frequency analyses in gas phase combined with basis sets Def2-SVP implemented in the Gaussian 09 package for all atoms.

Reaction Procedures

General synthetic procedure for benzophenones with different leaving group



Synthesis of 4-acetoxybenzophenone. Under nitrogen protection, a solution of 4-hydroxybenzophenone (2.42 g, 12 mmol), acetylchloride (1.28 mL, 18 mmol) and triethylamine (3.36 mL, 24 mmol) in dichloromethane (150 mL) was heated under reflux for 20 h. After cooling down to room temperature, the mixture was workup with H₂O for three times. The organic phase was dried over MgSO₄ and concentrated under reduced pressure and the residue was purified by column chromatography on silica gel (PE/EA =20/1-3/1) to give a white solid (2.19 g, 76%). ¹H NMR (400 MHz, CDCl₃): δ = 7.84–7.87 (2H, m), 7.79–7.81 (2H, m), 7.58–7.61 (1H, m), 7.47–7.50 (2H, m), 7.20–7.24(2H, m), 2.34 (3H, s); ¹³C NMR (101 MHz, CDCl₃): δ =195.6, 169.1, 154.0, 137.5, 135.2, 132.5, 131.3, 130.1, 128.5, 121.6, 21.3.

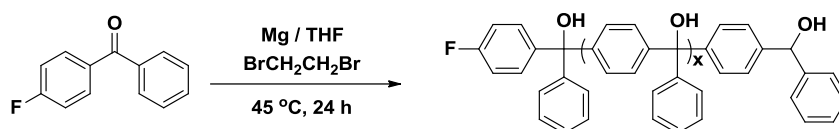


Synthesis of 4-benzoylphenyl tosylate. Under nitrogen protection, a solution of 4-hydroxybenzophenone (2.42 g, 12 mmol), p-toluenesulfonyl chloride (3.558g, 18 mmol) and triethylamine (3.36 mL, 24 mmol) in dichloromethane (150 mL) was heated under reflux for 20 h. After cooling down to room temperature, the mixture was workup with H₂O for three times. The organic phase was dried over MgSO₄ and concentrated under reduced pressure and the residue was purified by column chromatography on silica gel (PE/EA =20/1-3/1) to give a white solid (3.38 g, 80%). ¹H NMR (400 MHz, CDCl₃): δ = 7.81-7.70 (6H, t), 7.60-7.55 (1H, t), 7.50-7.43 (2H, t), 7.39–7.29 (2H, d), 7.13–7.09 (2H, d), 2.43 (3H, s); ¹³C NMR (101 MHz, CDCl₃): δ =195.31, 152.61, 146.01, 137.16, 136.28, 132.89, 131.86, 130.13, 128.51, 122.41, 21.8.

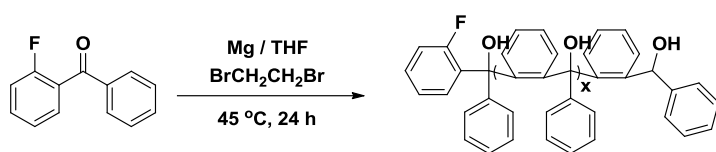


Synthesis of 4-benzoylphenyl triflate. Under nitrogen protection, a solution of 4-hydroxybenzophenone (1.12 g, 6.0 mmol), trifluoromethanesulfonyl chloride (1.52 g, 9.0 mmol) and triethylamine (1.68 mL, 12 mmol) in dichloromethane (70 mL) was heated under reflux for 20 h. After cooling down to room temperature, the mixture was workup with H₂O for three times. The organic phase was dried over MgSO₄ and concentrated under reduced pressure and the residue was purified by column chromatography on silica gel (PE/EA =20/1-3/1) to give a white solid (1.41 g, 72%). ¹H NMR (400 MHz, CDCl₃): δ = 7.94-7.89 (2H, d), 7.82-7.77 (2H, d), 7.68-7.60 (1H, t), 7.55-7.48 (2H, t), 7.45-7.37 (2H, d); ¹³C NMR (101 MHz, CDCl₃): δ =195.14, 152.10, 137.62, 136.51, 133.36, 132.25, 130.26, 128.47, 121.55; ¹⁹F NMR (376 MHz, CDCl₃): δ=-72.35.

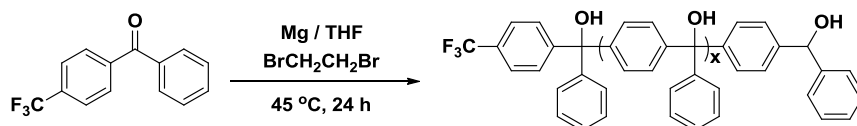
General synthetic procedure for self-condensing ketyl radical anion polymerization



Synthesis of fluoro-PTPM with 4-fluorobenzophenone. Under nitrogen protection, freshly peeled Mg scraps 0.144 g (6.0 mmol) was added into flame-dried Schlenk tube, then the solution of monomer which 4-fluorobenzophenone 1.0 g (5.0 mmol) dissolved in THF (10 mL) was injected into the tube with a syringe. After stirring for 10 min, 0.2 eq. 1, 2-dibromoethane was added to the Schlenk tube, and then reacted at 45 °C for 24 h. The reaction was quenched and hydrolysis by saturated aqueous ammonium chloride at room temperature, then workup with dichloromethane/ water. The organic solution was dried with anhydrous MgSO₄ and concentrated under reduced pressure. The oily liquids product was diluted with dichloromethane then precipitated with excessive petroleum ether for three times, after filtered and dried under vacuum, polymer was obtained as an off-white powder (yield: 70%). ¹H NMR (400 MHz, CDCl₃): δ=7.60-6.75 (broad, -phenyl), δ=3.83-3.35 (broad, -OH); ¹³C NMR (101 MHz, CDCl₃): δ=162.59, 160.66, 146.57, 145.18, 144.05-142.34, 140.18, 130.50-129.90, 128.79-125.22, 115.00-113.62, 82.84, 81.44; ¹⁹F NMR (376 MHz, CDCl₃): δ=(-115.32)-(-116.01); *M_{n, GPC}*=3400 g/mol, *D*=1.40; FT-IR (KBr pellets): Wavenumber=3670-3125 (O-H), 3120-3000 (Ar-H), 1620-1465 (phenyl), 1295-1250 (Ar-F), 1090-940 (C-O).

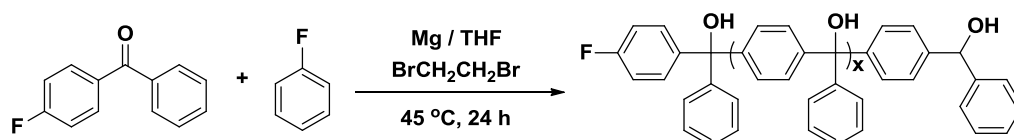


Synthesis of fluoro-PTPM with 2-fluorobenzophenone. Under nitrogen protection, freshly peeled Mg scraps 0.144 g (6.0 mmol) was added into flame-dried Schlenk tube, then the solution of 4-fluorobenzophenone 1.0 g (5.0 mmol) dissolved in THF (10 mL) was injected into the tube with a syringe. After stirring for 10 min, 0.2 eq. 1, 2-dibromoethane was added to the Schlenk tube, and then reacted at 45 °C for 24 h. The reaction was quenched and hydrolysis by saturated aqueous ammonium chloride at room temperature, then workup with dichloromethane/ water. The organic solution was dried with anhydrous MgSO₄ and concentrated under reduced pressure. The oily liquids product was diluted with dichloromethane then precipitated with excessive petroleum ether for three times, after filtered and dried under vacuum, polymer was obtained as an off-white powder (yield: 70%). ¹H NMR (400 MHz, CDCl₃): δ=7.85-6.64 (broad, -phenyl), δ=2.95-2.80 (broad, -OH); ¹³C NMR (101 MHz, CDCl₃): δ=145.51, 140.85, 129.15-125.34, 74.72; *M_{n,GPC}*=3800 g/mol, *D*=1.25; FT-IR (KBr pellets): Wavenumber=3710-3120 (O-H), 3100-3000 (Ar-H), 1630-1460 (phenyl), 1295-1250 (Ar-F), 1080-950 (C-O).

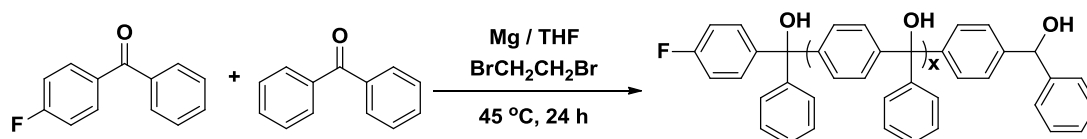


Synthesis of trifluoromethyl-PTPM with 4-trifluoromethylbenzophenone. Under nitrogen protection, freshly peeled Mg scraps 0.115 g (4.8 mmol) was added into flame-dried Schlenk tube, then the solution of 4-trifluoromethylbenzophenone 1.0 g (4.0 mmol) dissolved in THF (8 mL) was injected into the tube with a syringe. After stirring for 10 min, 0.2 eq. 1, 2-dibromoethane was added to the Schlenk tube, and then reacted at 45 °C for 24 h. The reaction was quenched and hydrolysis by saturated aqueous ammonium chloride at room temperature, then workup with dichloromethane/ water. The organic solution was dried with anhydrous MgSO₄ and concentrated under reduced pressure. The oily liquids product was diluted with dichloromethane then precipitated with excessive petroleum ether

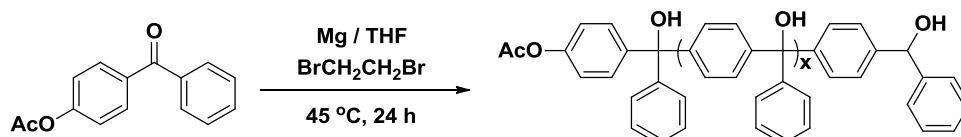
for three times, after filtered and dried under vacuum, polymer was obtained as an off-white powder (yield: 74%). ^1H NMR (400 MHz, CDCl_3): $\delta=7.82-6.73$ (broad, -phenyl), $\delta=3.38-2.85$ (broad, -OH); ^{13}C NMR (101 MHz, CDCl_3): $\delta=145.25, 137.52, 13.5.63, 133.41-125.36, 83.4$; ^{19}F NMR (376 MHz, CDCl_3): $\delta=-65.32$; $M_{n,\text{GPC}}=4900$ g/mol, $D=1.38$; FT-IR (KBr pellets): Wavenumber= $3622-3128$ (O-H), $3120-3000$ (Ar-H), $1755-1525$ (phenyl), $1045-958$ (C-O).



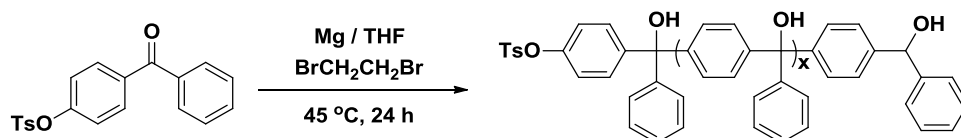
Synthesis of fluoro-PTPM with 4-fluorobenzophenone and fluorobenzene. Under nitrogen protection, freshly peeled Mg scraps 0.144 g (6.0 mmol) was added into flame-dried Schlenk tube, then the solution of monomer which 4-fluorobenzophenone 1.0 g (5.0 mmol) and fluorobenzene 0.48 g (5.0 mmol) dissolved in THF (10 mL) was injected into the tube with a syringe. After stirring for 10 min, 0.2 eq. 1, 2-dibromoethane was added to the Schlenk tube, and then reacted at 45 °C for 24 h. The reaction was quenched and hydrolysis by saturated aqueous ammonium chloride at room temperature, then workup with dichloromethane/ water. The organic solution was dried with anhydrous MgSO_4 and concentrated under reduced pressure. The oily liquids product was diluted with dichloromethane then precipitated with excessive petroleum ether for three times, after filtered and dried under vacuum, polymer was obtained as an off-white powder (yield: 68%). ^1H NMR (400 MHz, CDCl_3): $\delta=7.60-6.75$ (broad, -phenyl), $\delta=3.83-3.35$ (broad, -OH); ^{13}C NMR (101 MHz, CDCl_3): $\delta=162.59, 160.66, 146.57, 145.18, 144.05-142.34, 140.18, 130.50-129.90, 128.79-125.22, 115.00-113.62, 82.84, 81.44$; ^{19}F NMR (376 MHz, CDCl_3): $\delta=(-115.32)-(-116.01)$; $M_{n,\text{GPC}}=3300$ g/mol, $D=1.38$; FT-IR (KBr pellets): Wavenumber= $3670-3125$ (O-H), $3120-3000$ (Ar-H), $1620-1465$ (phenyl), $1295-1250$ (Ar-F), $1090-940$ (C-O).



Synthesis of fluoro-PTPM with 4-fluorobenzophenone and benzophenone. Under nitrogen protection, freshly peeled Mg scraps 0.144 g (6.0 mmol) was added into flame-dried Schlenk tube, then the solution of monomer which 4-fluorobenzophenone 1.0 g (5.0 mmol) and benzophenone 0.91 g (5.0 mmol) dissolved in THF (10 mL) was injected into the tube with a syringe. After stirring for 10 min, 0.2 eq. 1, 2-dibromoethane was added to the Schlenk tube, and then reacted at 45 °C for 24 h. The reaction was quenched and hydrolysis by saturated aqueous ammonium chloride at room temperature, then workup with dichloromethane/ water. The organic solution was dried with anhydrous MgSO₄ and concentrated under reduced pressure. Product can't be precipitated in petroleum ether and only trace polymer detected by NMR.

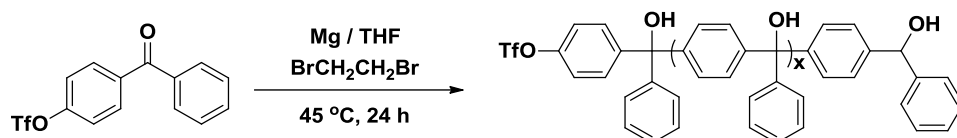


Synthesis of acetoxy-PTPM with 4-acetoxybenzophenone. Under nitrogen protection, freshly peeled Mg scraps 0.144 g (6.0 mmol) was added into flame-dried Schlenk tube, then the solution of monomer which 4-acetoxybenzophenone 1.2 g (5.0 mmol) dissolved in THF (10 mL) was injected into the tube with a syringe. After stirring for 10 min, 0.2 eq. 1, 2-dibromoethane was added to the Schlenk tube, and then reacted at 45 °C for 24 h. The reaction was quenched and hydrolysis by saturated aqueous ammonium chloride at room temperature, then workup with dichloromethane/ water. The organic solution was dried with anhydrous MgSO₄ and concentrated under reduced pressure. Product can't be precipitated in petroleum ether and no polymer detected by NMR.

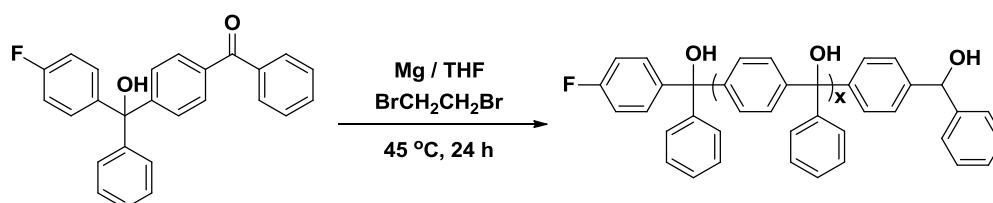


Synthesis of tosylate-PTPM with 4-benzoylphenyl tosylate. Under nitrogen protection, freshly peeled Mg scraps 0.144 g (6.0 mmol) was added into flame-dried Schlenk tube, then the solution of monomer which 4-benzoylphenyl tosylate 1.8 g (5.0 mmol) dissolved in THF (10 mL) was injected

into the tube with a syringe. After stirring for 10 min, 0.2 eq. 1, 2-dibromoethane was added to the Schlenk tube, and then reacted at 45 °C for 24 h. The reaction was quenched and hydrolysis by saturated aqueous ammonium chloride at room temperature, then workup with dichloromethane/ water. The organic solution was dried with anhydrous MgSO₄ and concentrated under reduced pressure. Product can't be precipitated in petroleum ether and no polymer detected by NMR.



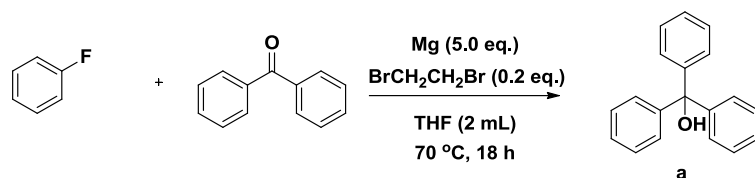
Synthesis of triflate-PTPM with 4-benzoylphenyl triflate. Under nitrogen protection, freshly peeled Mg scraps 0.144 g (6.0 mmol) was added into flame-dried Schlenk tube, then the solution of monomer which 4-benzoylphenyl triflate 1.65 g (5.0 mmol) dissolved in THF (10 mL) was injected into the tube with a syringe. After stirring for 10 min, 0.2 eq. 1, 2-dibromoethane was added to the Schlenk tube, and then reacted at 45 °C for 24 h. The reaction was quenched and hydrolysis by saturated aqueous ammonium chloride at room temperature, then workup with dichloromethane/ water. The organic solution was dried with anhydrous MgSO₄ and concentrated under reduced pressure. Product can't be precipitated in petroleum ether and no polymer detected by NMR.



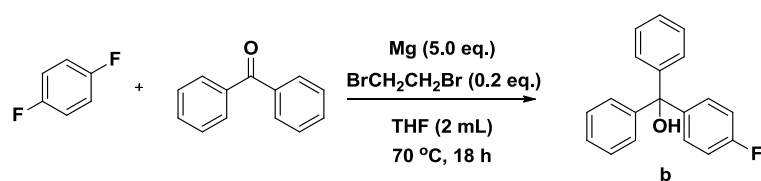
Polymerization procedure of dimer intermediate. Under nitrogen protection, freshly peeled Mg scraps 0.072 g (3.0 mmol) was added into flame-dried Schlenk tube, then the solution of monomer which dimer intermediate 0.96 g (2.5 mmol) dissolved in THF (10 mL) was injected into the tube with a syringe. After stirring for 10 min, 0.2 eq. 1, 2-dibromoethane was added to the Schlenk tube, and then reacted at 45 °C for 24 h. The reaction was quenched and hydrolysis by saturated aqueous ammonium chloride at room temperature, then workup with dichloromethane/ water. The organic solution was dried with anhydrous MgSO₄ and concentrated under reduced pressure. Product can't be precipitated in

petroleum ether and no polymer detected by NMR.

General synthetic procedure for the Barbier C-F activation reaction

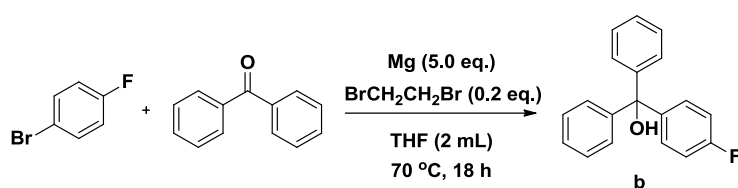


Barbier C-F Activation Reaction with fluorobenzene and benzophenone. Under nitrogen protection, freshly peeled Mg scraps 0.120 g (5.0 mmol) was added into flame-dried Schlenk tube, then the solution of reactant and additives which benzophenone 0.364 g (2.0 mmol), fluorobenzene 0.096 g (1.0 mmol) and 20 μ L of 1, 2-dibromoethane dissolved in THF (2 mL) was injected into the tube with a syringe. After the reaction was refluxed for 18 h, the solution was quenched and hydrolysis by 20 mL saturated aqueous ammonium chloride at room temperature, then workup with dichloromethane/water. The organic solution was dried with anhydrous MgSO₄ and concentrated under reduced pressure and the residue was purified by column chromatography on silica gel (PE/EA =20/1-3/1) to give 25% yield of a as a white solid. ¹H NMR (400 MHz, CDCl₃): δ 7.38–7.17 (m, 15H), 2.82 (s, 1H). ¹³C NMR (101 MHz, CDCl₃): 146.87, 127.98, 127.96, 127.31, 82.06, 77.39, 77.08, 76.76.

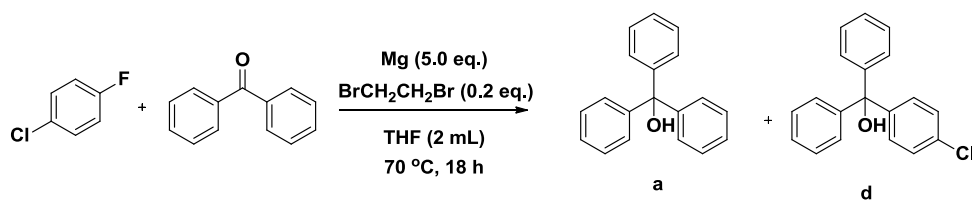


Barbier C-F Activation Reaction with 1,4-difluorobenzene and benzophenone. Under nitrogen protection, freshly peeled Mg scraps 0.120 g (5.0 mmol) was added into flame-dried Schlenk tube, then the solution of reactant and additives which benzophenone 0.364 g (2.0 mmol), 1,4-difluorobenzene 0.114 g (1.0 mmol) and 20 μ L of 1, 2-dibromoethane dissolved in THF (2 mL) was injected into the tube with a syringe. After the reaction was refluxed for 18 h, the solution was quenched and hydrolysis by 20 mL saturated aqueous ammonium chloride at room temperature, then workup with

dichloromethane/water. The organic solution was dried with anhydrous MgSO_4 and concentrated under reduced pressure and the residue was purified by column chromatography on silica gel (PE/EA =20/1-3/1) to give 29% yield of **b** as a white solid. ^1H NMR (400 MHz, CDCl_3): δ 7.39–7.22 (m, 12H), 6.98 (d, $J = 8.6$ Hz, 2H), 2.82 (s, 1H). ^{13}C NMR (101 MHz, CDCl_3): δ 163.16, 160.71, 146.73, 142.71, 129.79, 129.71, 128.64, 128.31, 128.14, 128.06, 127.85, 127.45, 127.32, 126.98, 126.78, 126.14, 126.02, 114.81, 114.60, 81.70. ^{19}F NMR (376 MHz, CDCl_3) δ -115.52.

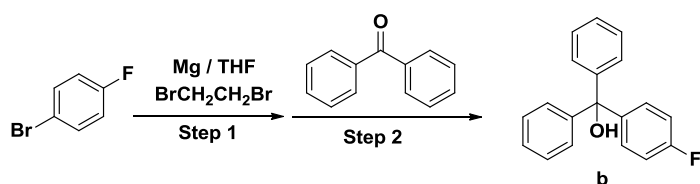


Barbier C-F activation reaction with 4-bromofluorobenzene and benzophenone. Under nitrogen protection, freshly peeled Mg scraps 0.120 g (5.0 mmol) was added into flame-dried Schlenk tube, then the solution of reactant and additives which benzophenone 0.364 g (2.0 mmol), 4-bromofluorobenzene 0.175 g (1.0 mmol) and 20 μL of 1, 2-dibromoethane dissolved in THF (2 mL) was injected into the tube with a syringe. After the reaction was refluxed for 18 h, the solution was quenched and hydrolysis by 20 mL saturated aqueous ammonium chloride at room temperature, then workup with dichloromethane/water. The organic solution was dried with anhydrous MgSO_4 and concentrated under reduced pressure and the residue was purified by column chromatography on silica gel (PE/EA =20/1-3/1) to give 36% yield of **b** as a white solid. ^1H NMR (400 MHz, CDCl_3): δ 7.39–7.22 (m, 12H), 6.98 (d, $J = 8.6$ Hz, 2H), 2.82 (s, 1H). ^{13}C NMR (101 MHz, CDCl_3): δ 163.16, 160.71, 146.73, 142.71, 129.79, 129.71, 128.64, 128.31, 128.14, 128.06, 127.85, 127.45, 127.32, 126.98, 126.78, 126.14, 126.02, 114.81, 114.60, 81.70. ^{19}F NMR (376 MHz, CDCl_3): δ -115.52.



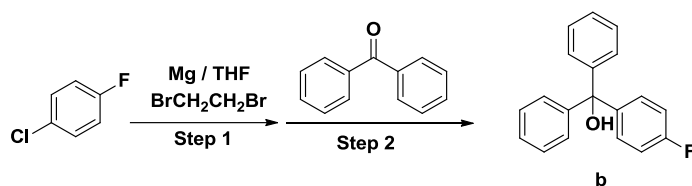
Barbier C-F activation reaction with 4-chlorofluorobenzene and benzophenone. Under nitrogen protection, freshly peeled Mg scraps 0.120 g (5.0 mmol) was added into flame-dried Schlenk tube, then the solution of reactant and additives which benzophenone 0.364 g (2.0 mmol), 4-chlorofluorobenzene 0.130 g (1.0 mmol) and 20 μL of 1, 2-dibromoethane dissolved in THF (2 mL) was injected into the tube with a syringe. After the reaction was refluxed for 18 h, the solution was quenched and hydrolysis by 20 mL saturated aqueous ammonium chloride at room temperature, then workup with dichloromethane/water. The organic solution was dried with anhydrous MgSO_4 and concentrated under reduced pressure and the residue was purified by column chromatography on silica gel (PE/EA =20/1-3/1) to give mixture of a and d as a white solid (a/d=1.7:2.3, determined by ^1H NMR, a=12% yield, d=16% yield). ^1H NMR (400 MHz, CDCl_3): δ 7.33–7.12 (m, 42H), 3.03 (s, 1.09H), 2.83 (s, 1H), 2.81 (s, 1.25H). ^{13}C NMR (101 MHz, CDCl_3): δ 146.86, 146.46, 145.36, 144.16, 133.17, 129.38, 128.62, 128.10, 128.05, 127.95, 127.83, 127.52, 127.31, 127.28, 126.97, 126.13, 83.04, 82.05, 81.69.

General synthetic procedure for the Grignard reaction with fluoro-compounds

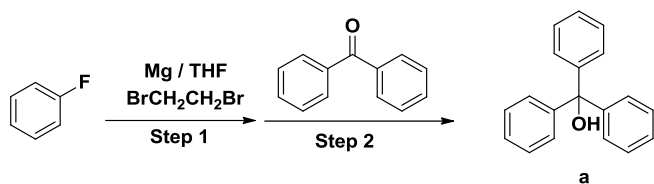


Grignard reaction with 4-bromofluorobenzene and benzophenone. Under nitrogen protection, freshly peeled Mg scraps 0.120 g (5.0 mmol) was added into flame-dried Schlenk tube, then the solution of fluoro-compounds which 4-bromofluorobenzene 0.175 g (1.0 mmol) dissolved in THF (2 mL) was injected into the tube with a syringe. After stirring for 10 min, 0.1 mL 1, 2-dibromoethane was added to the Schlenk tube, then refluxed for 2 h. Then the reaction solution was injected to benzophenone 0.364 g (2.0 mmol) which dissolved in THF (2 mL). After stirring for 24 h at room

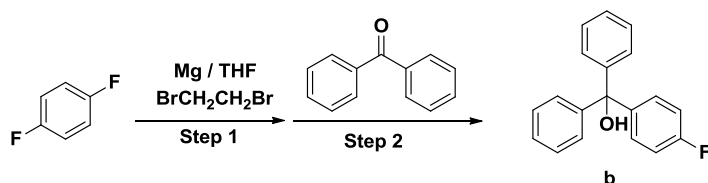
temperature, the reaction solution was quenched and hydrolysis by 20 mL saturated aqueous ammonium chloride, then workup with dichloromethane/water. The organic solution was dried with anhydrous MgSO_4 and concentrated under reduced pressure and the residue was purified by column chromatography on silica gel (PE/EA =20/1-3/1) to give 71% yield of **b** as a white solid. ^1H NMR (400 MHz, CDCl_3): δ 7.39–7.22 (m, 12H), 6.98 (d, J = 8.6 Hz, 2H), 2.82 (s, 1H). ^{13}C NMR (101 MHz, CDCl_3): δ 163.16, 160.71, 146.73, 142.71, 129.79, 129.71, 128.64, 128.31, 128.14, 128.06, 127.85, 127.45, 127.32, 126.98, 126.78, 126.14, 126.02, 114.81, 114.60, 81.70. ^{19}F NMR (376 MHz, CDCl_3) δ -115.52.



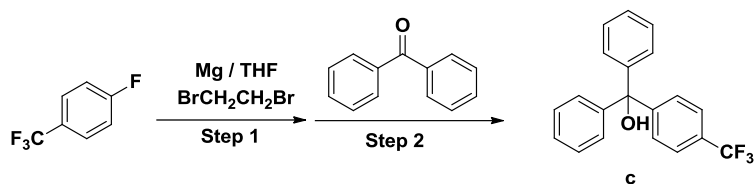
Grignard reaction with 4-chlorofluorobenzene and benzophenone. Under nitrogen protection, freshly peeled Mg scraps 0.120 g (5.0 mmol) was added into flame-dried Schlenk tube, then the solution of fluoro-compounds which 4-chlorofluorobenzene 0.130 g (1.0 mmol) dissolved in THF (2 mL) was injected into the tube with a syringe. After stirring for 10 min, 0.1 mL 1, 2-dibromoethane was added to the Schlenk tube, then refluxed for 2 h. Then the reaction solution was injected to benzophenone 0.364 g (2.0 mmol) which dissolved in THF (2 mL). After stirring for 24 h at room temperature, the reaction solution was quenched and hydrolysis by 20 mL saturated aqueous ammonium chloride, then workup with dichloromethane/water. The organic solution was dried with anhydrous MgSO_4 and concentrated under reduced pressure and the residue was purified by column chromatography on silica gel (PE/EA =20/1-3/1) to give 61% yield of **b** as a white solid. ^1H NMR (400 MHz, CDCl_3): δ 7.39–7.22 (m, 12H), 6.98 (d, J = 8.6 Hz, 2H), 2.82 (s, 1H). ^{13}C NMR (101 MHz, CDCl_3): δ 163.16, 160.71, 146.73, 142.71, 129.79, 129.71, 128.64, 128.31, 128.14, 128.06, 127.85, 127.45, 127.32, 126.98, 126.78, 126.14, 126.02, 114.81, 114.60, 81.70. ^{19}F NMR (376 MHz, CDCl_3) δ -115.52.



Grignard reaction with fluorobenzene and benzophenone. Under nitrogen protection, freshly peeled Mg scraps 0.120 g (5.0 mmol) was added into flame-dried Schlenk tube, then the solution of fluoro-compounds which fluorobenzene 0.096 g (1.0 mmol) dissolved in THF (2 mL) was injected into the tube with a syringe. After stirring for 10 min, 0.1 mL 1, 2-dibromoethane was added to the Schlenk tube, then refluxed for 2 h. Then the reaction solution was injected to benzophenone 0.364 g (2.0 mmol) which dissolved in THF (2 mL). After stirring for 24 h at room temperature, the reaction solution was quenched and hydrolysis by 20 mL saturated aqueous ammonium chloride, then workup with dichloromethane/water. The organic solution was dried with anhydrous MgSO₄ and concentrated under reduced pressure. The product was not detected by TLC and GC-MS.

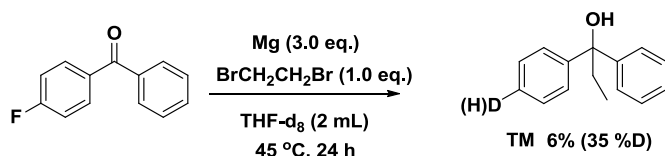


Grignard reaction with 1,4-difluorobenzene and benzophenone. Under nitrogen protection, freshly peeled Mg scraps 0.120 g (5.0 mmol) was added into flame-dried Schlenk tube, then the solution of fluoro-compounds which 1, 4-difluorobenzene 0.114 g (1.0 mmol) dissolved in THF (2 mL) was injected into the tube with a syringe. After stirring for 10 min, 0.1 mL 1, 2-dibromoethane was added to the Schlenk tube, then refluxed for 2 h. Then the reaction solution was injected to benzophenone 0.364 g (2.0 mmol) which dissolved in THF (2 mL). After stirring for 24 h at room temperature, the reaction solution was quenched and hydrolysis by 20 mL saturated aqueous ammonium chloride, then workup with dichloromethane/water. The organic solution was dried with anhydrous MgSO₄ and concentrated under reduced pressure. The product was not detected by TLC and GC-MS.



Grignard reaction with 4-fluorobenzotrifluoride and benzophenone. Under nitrogen protection, freshly peeled Mg scraps 0.120 g (5.0 mmol) was added into flame-dried Schlenk tube, then the solution of fluoro-compounds which 4-fluorobenzotrifluoride 0.114 g (1.0 mmol) dissolved in THF (2 mL) was injected into the tube with a syringe. After stirring for 10 min, 0.1 mL 1, 2-dibromoethane was added to the Schlenk tube, then refluxed for 2 h. Then the reaction solution was injected to benzophenone 0.364 g (2.0 mmol) which dissolved in THF (2 mL). After stirring for 24 h at room temperature, the reaction solution was quenched and hydrolysis by 20 mL saturated aqueous ammonium chloride, then workup with dichloromethane/water. The organic solution was dried with anhydrous MgSO_4 and concentrated under reduced pressure. The product was not detected by TLC and GC-MS.

General Procedure for Experimental Mechanistic Studies



Synthesis of fluoro-PTPM with 4-fluorobenzophenone in THF- d_8 . Under nitrogen protection, freshly peeled Mg scraps 0.144 g (6.0 mmol) was added into flame-dried Schlenk tube, then the solution of 4-fluorobenzophenone 0.4 g (2.0 mmol) dissolved in dry THF- d_8 (2 mL) was injected into the tube with a syringe. After stirring for 10 min, 1 eq. of 1, 2-dibromoethane was added to the Schlenk tube, and then reacted at 45 °C for 24 h. The reaction was quenched and hydrolysis by saturated aqueous ammonium chloride at room temperature, then workup with dichloromethane/water. The organic solution was dried with anhydrous MgSO_4 and concentrated under reduced pressure and then the residue was purified by column chromatography on silica gel (PE/EA =20/1-3/1) to give 6% yield of para-deuterated diphenylethylmethanol as a white solid. ^1H NMR (600 MHz, Acetone- d_6) δ 7.48–

7.45 (m, 4H), (dd, J = 8.4, 1.1 Hz, 4H), 7.26–7.21 (m, 4H), 7.14–7.10 (m, 1.65H), 4.35 (s, 1H), 2.31 (q, J = 7.3 Hz, 2H), 0.82 (t, J = 7.3 Hz, 3H). ¹³C NMR (151 MHz, Acetone-*d*₆): δ 148.32, 127.71, 126.13, 77.33, 34.15, 7.67. HRMS (EI⁺) calcd for [C₁₅H₁₅DO]⁺ (M⁺):213.1264, found: 213.1274.